

Interlinking diatom frustule diversity from the abyss of the central Arabian Sea to surface processes: physical forcing and oxygen minimum zone

Medhavi Pandey^{1,2}, Haimanti Biswas^{1,2,*}, Mintu Chowdhury^{1,3}

¹CSIR National Institute of Oceanography, Biological Oceanography Division,
Dona Paula, Goa 403004. India.

²Academy of Scientific and Innovative Research (AcSIR), Ghaziabad-201002, India

³School of Oceanographic Studies, Jadavpur University, Kolkata, West Bengal, India

*Corresponding author: haimanti.biswas@nio.org; haimanti.biswas.nio@gmail.com

Abstract: This study analyzed the diversity and abundance of diatom frustules including the ancillary parameters using the core top sediments from five locations (21, 19, 15, 13, and 11 °N) along the central Arabian Sea (64 °E), an area profoundly influenced by atmospheric forcing (monsoons) and oxygen minimum zone (OMZ) with high spatial variability. Significantly higher organic carbon ($0.97\pm 0.05\%$) and diatom frustules ($5.92\pm 0.57 \times 10^4$ valves g^{-1}) were noticed in the north (21, 19, 15 °N) where natural nutrient enrichment via open-ocean upwelling, winter convection, and lateral advection support large diatom-dominated phytoplankton blooms and intense OMZ. Conversely, the south (13, 11 °N) depicted significantly lower organic carbon ($0.74\pm 0.08\%$) as well as frustules ($4.02\pm 0.87 \times 10^4$ valves g^{-1}) as this area mostly remains nutrient-poor dominated by small-medium sized phytoplankton. The north was dominated by large-sized diatoms like *Coscinodiscus* that could escape grazing and sink consequently due to higher ballasting. Furthermore, the presence of the intense OMZ in the north might reduce grazing pressure (low zooplankton stock) and mineralization speed facilitating higher phytodetritus transport. Relatively smaller chain-forming centric (*Thalassiosira*) and pennate diatoms (*Pseudo-nitzschia*, *Fragilaria*, *Nitzschia*, etc.) were found throughout the transect with higher abundance in the south. The euphotic diatom diversity from the existing literature was compared with the frustule diversity from the sediments suggesting not all diatoms make their way to the abyss. Such distinct spatial north-south variability in diatom frustule size as well as abundance could be attributed to cell size, grazing, and water column mineralization rates related to OMZ.

Keywords: Phytoplankton; Diatoms; Carbon export; *Coscinodiscus*; *Thalassiosira*; Arabian Sea; Physical forcing

1. Introduction

Marine phytoplankton play a key role in modulating the global carbon cycle by fixing ~50% of the atmospheric CO₂ as organic matter in the euphotic zone (Field et al. 1998; Behrenfeld et al. 2006). A small fraction of this organic matter (large and dense phytodetritus) sinks (Le Moigne, 2019) to the ocean interior (Buesseler, 1998) where it gets stored for hundreds of years. This process is termed marine Biological Carbon Pump (BCP) (Volk and Hoffert, 1985). The strength of the organic matter export flux from the upper euphotic zone to the lower mesopelagic region depends on the remineralization of organic matter which is controlled by oxygen concentrations, temperature, phytoplankton cell size and community composition, zooplankton abundance and activity, organic matter stoichiometry, and the fractionation of particulate to dissolved organic carbon (POC/DOC) (Marsay et al. 2015; Keil et al. 2016; Cavan et al. 2017; Engel et al. 2017). Productive oceanic areas are likely to be associated with high organic matter export flux to the sediment as has been noticed in some shallow coastal areas after phytoplankton bloom (Abrantes et al. 2016). However, even in the shelf regions, high organic matter remineralization/oxidation may remove nearly 80-90% of the spring bloom (Falkowski et al. 1988). Likewise, many studies indicated that the upper ocean productivity was inversely correlated with export flux to the lower mesopelagic (Francois et al. 2002; Ragueneau et al. 2006; Mouw et al. 2016). Out of multiple factors controlling the efficacy of the BCP, phytoplankton community composition (that controls organic matter stoichiometry) as well as the presence of well-oxygenated water (Keil et al. 2016) are important for efficient mineralization of the organic matter by marine microbial consortia.

Among the photosynthetic microphytoplankton, diatoms dominate all oceanic productive areas and contribute ~20% to the global primary production and 40% to total marine primary production (Nelson et al. 1995; Field et al. 1998). Diatoms are efficient carbon exporters mostly due to their siliceous frustules that provide excellent ballasting with easy export of carbon to the deep sea (Tréguer et al. 2018). The sinking of diatoms is a major component of the global carbon cycle (Du Clos et al, 2021). It has also been estimated that they contribute ~50% to POC export flux (Jin et al. 2006; Tréguer and De La Rocha, 2013) which if reaches the abyssal plain can be stored at least for centuries (Tréguer et al. 2018; Le Moigne, 2019). Some authors reported that the loose packaging of the diatom-dominated organic matter can be more labile for microbial degradation and therefore, less efficient for export (Francois et al. 2002; Alonso-González et al. 2010). On the contrary, it was observed in an experimental study that diatom-dominated phytodetritus exhibited higher resistance to microbial degradation relative to non-diatom dominated organic matter (Cabrera-Brufau et al. 2021). There are studies correlating phytoplankton bloom and export flux with sediment trap samples. Rixen et al. (2019a) noticed large diatom dominated opal flux in the central Arabian Sea after the summer monsoon

(nutrient-enriched) whereas, the dominance of calcifying coccolithophore flux during the intermonsoon (nutrient-poor). However, there are very less studies that correlated the upper ocean phytoplankton bloom with the phytodetritus that is collected from the seabed, particularly from the open ocean regions.

Furthermore, the presence and absence of oxygen-deficient waters below the euphotic zone control the efficiency of organic matter mineralization/export to the sediment (Francois et al. 2002; Keil et al. 2016). Several studies support the good preservation of organic carbon in anoxic waters as the possibility of anoxic degradation becomes sufficiently slower or less comprehensive relative to oxic carbon remineralization (Keil et al. 2016). The Arabian Sea also hosts a persistent oxygen minimum zone (OMZ) present within 150 to 1200 m (Wyrski, 1971; Banse et al. 2014) in the central and northeastern parts (Naqvi, 1987) mostly due to high primary production and poor ventilation of sub-surface waters. Therefore, may considerably impact the magnitude of carbon degradation, export, and storage (Cavan et al. 2017). Some earlier studies from the Arabian Sea suggested a direct flux of fresh phytoplankton-derived organic matter from the euphotic to bathypelagic zones (Pfannkuche et al. 2000). Roman et al. (2000) found no link between POC flux and mesozooplankton fecal matter suggesting that phytodetritus may sink directly. Importantly, within the OMZ the mesozooplankton standing stock is usually less and may slow down the process of defragmentation and further degradation by microbes letting relatively higher organic matter reach the sediment (Cavan et al. 2017). The central Arabian Sea in its northern part hosts the most prominent OMZ (Banse et al. 2014; Naqvi et al. 1987) which slowly disappears towards the south (Shenoy et al. 2021). It was shown by Keil et al. (2016) using a multiple proxy approach and model that the spatial variability of OMZ in the Arabian Sea directly impacts phytodetritus transport to the sediment. Previous observations of particle export flux using the sediment traps from the Arabian Sea are available from the Joint Global Ocean Flux Studies (JGOFS) program highlighting the dominance of opal or diatom-dominated organic matter (Haake et al. 1993; Rixen et al. 2019a). Our recent observations (Chowdhury et al. 2021; Silori et al. 2021) from the central Arabian Sea documented the occurrences of diatom-dominated phytoplankton bloom and its close coupling with particulate organic matter (POM) dynamics within the euphotic zone during the southwest monsoons (2017-2018). In the present study, we examined the utility of surface sediment diatom frustules as a proxy for the upper ocean phytoplankton blooms from five sites in the central Arabian Sea. Radiolarians were also quantified as an indicator of microzooplankton.

2. Materials and methods

2.1. Sample collection

Short sediment cores were collected onboard *RV. Sindhu Sadhana* (SSD-068) from 5 locations (21, 19, 15, 13, and 11 °N) from the central Arabian Sea (along 64 °E) (Fig.1) during Dec 2019- Jan 2020. The water depths in the sampling locations ranged between 3388-4320 m (Fig. 1). The cores were collected using an Ocean Scientific International Limited Maxi Multi-corer (600 mm long core tubes, 110 mm outer diameter, and 100 mm inner diameter). Immediately after collection, the cores were subsampled vertically at every 0.5 cm interval using a plate and ring and stored in clean plastic containers at 4 °C in the dark until further analyses. For the present study, the topmost part (0.5 cm surface layer) of the core (undisturbed sediment) has been studied. The samples were processed and total carbon (TC), total inorganic carbon (TIC), and total nitrogen (TN) contents were measured. As a proxy of phytoplankton, diatom frustules were counted and enumerated.

2.2. Analytical method

2.2.1. Sedimentary total inorganic carbon (TIC), total organic carbon (TOC), and total nitrogen (TN) contents

Oven-dried sediments (60 °C for 48 h) were homogenized by grinding on agate mortar and pestle and stored in clean vials for further analysis. For analyzing total carbon and nitrogen (TC and TN) 10 mg dried, crushed, and homogenized sediment samples were taken and measured using a CHN Elemental analyzer (Euro Vector EA3000 series analyzer, CAF) against a soil reference material NC (Thermofisher Scientific, Cambridge, UK) with an analytical error < 2%. TIC contents were analyzed using a coulometer attached to an acidification module (Model CM5015) against the calcium carbonate standard (Merck, Germany). The accuracy of the measurements was within 0.99. TOC was obtained as the difference between total carbon and total inorganic carbon (TOC=TC-TIC).

2.2.2. Analysis of diatom frustules from sediments

Aliquots of 50 mg dried subsamples were taken in a 15 mL clean polypropylene tube followed by consecutive treatments with 10% HCl, 30% H₂O₂, and 0.01 N anhydrous sodium diphosphate (Na₄P₂O₇) to remove carbonates, organic matter, and fine clay particles (Armbrecht et al. 2018) respectively. The treated samples were then thoroughly rinsed with Milli- Q water three times. Finally, the tubes were filled with 10 mL Milli-Q water and gently mixed. An aliquot of 1 mL from this solution was analyzed in a Sedgewick rafter counting chamber (Pyser, UK) under an inverted microscope (Nikon Ti2) at 400× magnification using identification keys from Tomas, 1997; <http://www.algaebase.org>, <https://www.marinespecies.org/>. In this process, centrifugation was

avoided to prevent any breakage of frustules (Koizumi and Tanimura, 1985), and fragments of size more than half were considered as a whole (Abrantes and Sancetta, 1985). The diatom abundance was expressed as valves g^{-1} dry sediment.

2.2.3. Statistical analysis

After checking the normality and variance of the data sets, Single-factor Analysis of Variance (ANOVA) was used in Microsoft Excel for comparing the sites for the significance of differences ($p < 0.05$ was taken as significant).

3. Results

Based on the organic carbon and frustule abundance, we have categorized the stations as north (21, 19, and 15 °N) and south (13 and 11°N).

3.1. Inorganic and organic carbon and total nitrogen contents

The TIC contents (Fig. 2A, Table 1) in the surface sediments of the northern stations were 5.08 ± 1.56 % and increased by 1.4 times ($p < 0.05$) in the south. The % of TOC (Fig. 2B) was nearly 7 times lower than the TIC and revealed a reversed trend with increasing ($p < 0.05$) values in the north and decreasing steadily towards the south (Fig. 2B). The southernmost stations (13 and 11°N) had the lowest TOC value (0.7%) while the station in the north (21°N) showed a maximum of 1.0% ($p < 0.05$). The TN contents (Fig. 2C; Table 1) ranged between 0.06% and 0.11% without any significant variability ($p > 0.05$, Table 2).

3.2 Diatom frustule abundance, composition, and distribution

A high number of diatom frustules (Fig. 2D) were observed in the microscopy ranging from 3.29 to 6.50×10^4 valves g^{-1} . The highest diatom frustule density (6.50×10^4 valves g^{-1}) was observed at 19 °N, followed by 21 °N (5.92×10^4 valves g^{-1}), and became half (3.29×10^4 valves g^{-1}) at 11 °N ($p < 0.05$) (Table 1). Some of the microscopic photographs of the diatom frustules are shown in Supplementary Fig. 1. The Shannon-Wiener diversity index (H') (Fig. 3A) showed low variability with an average value of 1.57 ± 0.22 . The highest diversity was encountered at the northernmost station (21 °N) with an H' value of 1.93 while the least at the southernmost station (13 °N) with 1.35, with no significant difference between the stations ($p > 0.05$). The average distribution of the major contributing species for all five stations has been presented in Fig. 1. A total of 23 genera of diatoms including 9 centric and 14 pennate were documented (Table 2). Two major dominating centric diatoms i.e. *Coscinodiscus* and *Thalassiosira* were the most frequently occurring in all stations. A clear trend of

increasing large centric diatom frustules like *Coscinodiscus* was noticed towards the northern side ($p < 0.05$) and a reverse trend was documented for *Thalassiosira* ($p < 0.05$).

Based on the existing literature (Karnan et al. 2020), diatom frustules were classified into three size classes (1) $< 30 \mu\text{m}$ as small, (2) $30\text{-}60 \mu\text{m}$ as a medium, and (3) $> 60 \mu\text{m}$ as large frustules (Fig. 3B; Table 1). A noticeable shift in diatom frustule distribution was noted from north to south with medium and large diatoms dominating the north while small diatoms dominated the south. The large frustules on average accounted for $\approx 40\%$ of the total distribution and dominated the northernmost station (21°N) with a valve density of $2.94 \times 10^4 \text{ g}^{-1}$ and the minimum contribution was found at the southernmost station (11°N) ($1.33 \times 10^4 \text{ valves g}^{-1}$) ($p < 0.05$). Medium sized-frustules dominated all the stations except at 21°N and accounted for nearly 49% on average with the highest abundance at 19°N ($3.26 \times 10^4 \text{ valves g}^{-1}$) and the lowest at 11°N ($1.52 \times 10^4 \text{ valves g}^{-1}$). The smallest size class contributed the least with an overall average of 12% in distributing spatially in the central Arabian Sea, and their number varied from 0.45 to $0.76 \times 10^4 \text{ valves g}^{-1}$ without any statistically significant difference between the stations.

Interestingly, centric diatoms number remained fivefold higher than pennate diatoms ($p < 0.05$) and they dominated all stations with a decreasing trend towards the south (Fig. 3C), however, pennate diatoms did not show any clear trend ($p > 0.05$). Out of the all size classes, the large-sized ($> 60 \mu\text{m}$) *Coscinodiscus* frustule was found in all stations, however, the highest number was observed at the north with nearly $1.33 \times 10^4 \text{ valves g}^{-1}$ frustules on average and decreased by 1.8 times ($p < 0.05$) in the southern stations ($13\text{-}11^\circ\text{N}$) (Fig. 3D, Table 1). *Thalassiosira* frustule (Fig. 3E) abundance ranged between $1.26\text{-}2.37 \times 10^4 \text{ valves g}^{-1}$ without any significant variability ($p > 0.05$) within the stations. The medium and small-size frustules did not reveal any statistically significant difference ($p > 0.05$), however, the large-sized frustules showed the highest abundance towards the south ($p < 0.05$). We have also counted the radiolarian abundance from the same samples and it showed significantly ($p < 0.05$) higher values in the south compared to the north (Fig. 3F).

4. Discussion

The export of organic matter to the sediment is governed by upper-ocean productivity in the entire north Indian Ocean (Rixen et al. 2019b). Particle flux ($1.3\text{-}3.3 \text{ g C m}^{-2} \text{ y}^{-1}$) recorded from this area is one of the highest compared to the other tropical and subtropical regions (Haake et al. 1993). The measured sedimentation rates in the central Arabian Sea (Prell et al. 1980; Ramaswamy et al. 1991) vary from $1.03\text{-}1.8 \text{ cm kyr}^{-1}$, and thus the top 0.5 cm of the core is likely to represent the recent past. In general, in the open ocean regions, the speed of phytodetritus flux can vary from $100\text{-}150 \text{ m d}^{-1}$ (Lampitt, 1985), and accordingly, it may take nearly one to two months to reach the abyssal floor

in the Arabian Sea. The mass sinking of diatoms is usually noticed when nutrients are exhausted (Smetacek, 1985; Krause et al. 2019). In a previous shallow sediment trap study from the coastal Arabian Sea, it was noticed that a higher flux of diatoms was associated with nutrient exhaustion during the intermonsoon season (Bhaskar et al. 2000). The summer monsoon-induced phytoplankton bloom usually terminates in September in the Arabian Sea and the samples from the present study were collected at the end of December. Consequently, the phytodetritus can be expected to reach the seabed within two months the organic matter collected from the surface sediment would contain the signature of the fresh bloom. The presence of fresh phytodetritus (intact cells of diatoms and cyanobacteria) was documented on the seabed at a depth of >4000 m from many oceanic regions (Smith et al. 1996; Agustì et al. 2015). Likewise, in a previous study direct flux of fresh phytodetritus from the euphotic to bathypelagic zones was reported from the Arabian Sea (Pfannkuche et al. 2000).

In the Arabian Sea, the presence of diatom-rich organic matter from the sediment trap samples indicated nutrient enrichment facilitated diatom bloom with consequent POC export flux (Rixen et al. 2019a) during the summer and winter monsoons (Nair et al. 1989; Haake et al. 1993; Rixen et al. 1996). Our results confirm the fact that diatoms play a key role in organic carbon export to the bathypelagic zone and the variability in upper ocean productivity is also reflected in diatom frustule abundance. However, the present observation also suggested a distinct north-south variability in sedimentary diatom frustule type and size class that has not been addressed previously. However, this would be interesting to compare the diatom community that is usually seen in the euphotic zone with the frustules found on the surface sediment as their sinking can be controlled by several factors. In the following sections, we discussed 1) the impacts of physical forcings on such north-south variability in diatom frustule diversity, size classes, and abundance, 2) the possible reasons for the observed mismatch between the euphotic diatom community and sedimentary frustules 3) the influence of the presence of OMZ.

4.1 Impacts of atmospheric forcing on diatom diversity, cell size, and sinking potential in the central Arabian Sea

The biogeochemistry of the Arabian Sea is largely influenced by the monsoonal reversal and is one of the most productive regions in the global oceans (Haake et al. 1993). Nutrient supply to the surface and consequent development of phytoplankton bloom in this region is directly controlled by prominent ocean-atmospheric coupling (Bhattathiri et al. 1996; Sawant and Madhupratap, 1996; Chowdhury et al. 2021; Silori et al. 2021). During the winter monsoon, the cold dry wind leads to winter cooling and subsequent convective mixing (Banse and McClain, 1986; Madhupratap et al. 1996) followed by the development of diatom-dominated phytoplankton bloom in the northern

Arabian Sea (Padmakumar et al. 2017; Chndrasekhararao et al. 2018; Sridevi and Sarma, 2022). During the summer monsoon, a low-level atmospheric Jet (Findlater Jet, Findlater, 1971) blows perpendicular to the Somalia coast (Fig. 1), and north of this jet axis, open-ocean upwelling occurs due to the positive wind stress curl (Smith and Bottero, 1977; Bauer et al. 1991) and makes the surface waters nutrient-enriched (Brink et al. 1998; Chowdhury et al. 2021). Downwelling occurs in the southern part of the jet axis and low nutrient levels prevail (Prasannakumar et al. 2001). More than 4 μM nitrate+nitrite levels (Supplementary Table 1) were recorded from the upwelling impacted regions of the northern part of the central Arabian Sea. High primary productivity ($1.7 \text{ g C m}^{-2} \text{ d}^{-1}$) (Prasannakumar et al. 2001), as well as large diatom-dominated phytoplankton blooms (Brock and McClain, 1992, Sawant and Madhupratap, 1996; Bhattathiri et al. 1996; Sawant and Madhupratap, 1996; Chowdhury et al. 2021), have been reported from this region. Because of this, the northern Arabian Sea remains productive most of the time of the year compared to the southern nutrient-poor region and is likely to receive a higher amount of phytodetritus to the sediment as has been observed in the present study. The open ocean regions usually show TOC <1% (Paropkari et al. 1992) due to increasing water depths (Suthhof et al. 2000) and our results are consistent with these trends. TN contents showed relatively lower values reported from the shelf regions, however, the deep-sea sediments from the Central Arabian Sea also exhibited similar values (0.06 -0.07%) (Suthhof et al. 2000) as observed in this study.

Large centric diatoms like *Rhizosolenia* sp., *Chaetoceros* sp., and *Coscinodiscus radiatus* (Garrison et al. 1998; Tarran et al. 1999; Chowdhury et al. 2021) have been noticed in the open ocean upwelling influenced regions. As diatoms are obligatory silicifiers, their ecophysiology is directly dependent on the dissolved silicate (DSi) levels (Smetacek, 1985). It has been noticed that in addition to nitrogen availability, DSi also plays an important role in controlling the development of diatom bloom in the Arabian Sea (Anju et al. 2020). The large cells require a high DSi supply for cell division and they usually thrive in nutrient-enriched waters. The large (>60 μm) and medium-sized (30 -60 μm) frustules were mostly noticed in the northern side which is usually associated with higher DSi supplies due to upwelling and winter convection. The study by Chowdhury et al. (2021) noticed depleted DSi levels ($\approx 1.5 \mu\text{M}$) towards the north and axis of Findlater Jet coupled with the abundance of large diatom blooms containing *Rhizosolenia* and *Coscinodiscus*. There was a clear succession in frustule, particularly, the occurrence of large diatoms like *Coscinodiscus* (> 60 μm) was mostly confined towards the north (Fig. 3D) and the maximum size was noticed ($\approx 200 \mu\text{m}$) from this region. Likewise, Rixen et al. (2019a) reported a high abundance of *Rhizosolenia*-dominated opal flux in the deep sediment trap ($\approx 3000 \text{ m}$) from the central Arabian Sea.

Along the axis of the Findlater Jet, between 15–17° N, high productivity values (1–1.7 g C m⁻² d⁻¹) were observed (Prasannakumar et al. 2001) this area is influenced by the lateral advection as well as entrainment which brings nutrients from the western Arabian Sea (Banse, 1987; Silori et al. 2021). The signature of $\delta^{15}\text{N}$ of particulate nitrogen (which is mostly autochthonous) along the axis of Findlater Jet also indicated that the source of nitrogen was likely to be from the western Arabian Sea coastal upwelling region (Silori et al. 2021). This should be also mentioned that the dissolved organic matter, as well as nutrients, are advected from the western Arabian Sea towards the central part, but the chances of diatom frustules being transported could be less due to their high ballasting. The study by Silori et al. (2021) also found mostly the signature of in situ produced organic matter in this region ruling out the possibility of the contribution of advected frustules from the coastal upwelling regions.

As mentioned earlier, the southern part of the jet axis remains nutrient-poor due to downwelling (Prasannakumar et al. 2001). Nearly 2 μM nitrate+nitrite levels were detected within the upper 60 m water column during the summer monsoons of 2017 and 2018 (Supplementary Table 1). Tarran et al. (1999) noticed <1 μM DSi was within 80 m of the water column from the southern stations at end of the summer monsoon as well intermonsoon. Prasannakumar et al. (2001) have reported moderate productivity (0.8 g C m⁻² d⁻¹) and attributed it to the lateral advection of nutrient-rich upwelled waters from the Somalia coast. And at these stations, the smaller chain-forming diatoms such as *Thalassiosira*, *Pseudo-nitzschia* sp., *Nitzschia closterium*, and dinoflagellates like *Gymnodinium* and *Gyrodinium* (Garrison et al. 1998; Tarran et al. 1999; Chowdhury et al. 2021) grow under low DSi levels. As it was observed that the small and medium-sized frustules (e.g. *Thalassiosira*) were found throughout the transect as they can sustain both low and high DSi levels due to a high surface area to volume ratio (Marañón et al. 2015) that facilitates efficient nutrient uptake. Undetectable nitrate was reported from the central Arabian Sea within the top 40 m water column during the spring intermonsoon (Prasannakumar and Narvekar, 2005). Calcifying nanophytoplankton like coccolithophores also contributes significantly to POC export and is noticed before the opal-dominated flux (Rixen et al. 2005) suggesting that during intermonsoon when low nutrient condition prevails nanoplankton may dominate the carbon export flux (Mergulhao et al. 2006). The southern stations repeatedly reported high dominance of nanoplanktonic coccolithophores from the sediment trap samples as well as from the surface sediments (Andruleit et al. 2000; Mergulhao et al. 2006) and hence justify higher TIC values compared to the north (Table 1). Similarly, small-celled diatoms may also dominate the low-nutrient region and contribute to carbon export flux (Leblanc et al. 2018) as evident from the frustule distribution from the southern stations. The particulate organic matter in the upper water column during the summer monsoon in the south showed less inter-annual variability (Rixen et al. 2019a) and lower

values than in the north (Silori et al. 2021) and is also consistent with the organic carbon content observed in the sediment.

We have compared the dominating diatom species from the euphotic layers using literature (Sawant and Madhupratap, 1996; Garrison et al. 1998; Tarran et al. 1999; Chowdhury et al. 2021) from the nearby locations to our sampling stations (Supplementary Table 2) and it revealed that the large centric diatoms (*Coscinodiscus*, *Rhizosolenia*, *Chaetoceros*, and *Proboscia alata*) dominated the open-ocean upwelling regions as well as the axis of the Findlater Jet. The assemblages of the small pennate diatoms (*Pseudo-nitzschia* and *Nitzschia closterium*) were observed in the low-nutrient offshore region of the central Arabian Sea (Garrison et al. 1998). Diatom cell size directly influences sinking velocities (Buesseler and Boyd, 2009) of the particles and marine BCP (Tréguer et al. 2018) as the larger cells sink faster. Similarly, in the north, large diatoms are expected to sink efficiently to the seabed compared to the smaller cells in the south.

4.2 The possible reasons for the observed mismatch between the euphotic diatom community and sedimentary frustules

The summary results of the diatom community from the north and south (Fig. 4 A-B) obtained from our previous study within the upper water column (Chowdhury et al. 2021) have been compared with the average diatom frustules from the surface sediments (Fig. 4C, 4D). Interestingly, the relative contributions of diatom frustules found on the seafloor partly match, but do not reflect the exact upper water column community composition suggesting that all frustules may not be transported from the upper water column to the abyss. The transport of diatom frustules from the euphotic zone to the seabed is dependent on some key factors including grazing by zooplankton as well as benthic fauna, degradation and dissolution of frustules, water depth, and the presence of oxygen. In the northern part of the central Arabian Sea, enrichment of nutrients, particularly DSi promotes large diatom growth with thick frustules and these characteristics help them to prevent grazing. Besides, the thicker frustules (e.g. *Coscinodiscus* and *Thalassiosira*) increase the resistance against grazing and preservation in the sediment compared to the thin frustules (e.g. *Chaetoceros* and *Skeletonema*) (Ryderheim et al. 2022). It has been observed in the experiment that the thicker and harder diatom cells like *Thalassiosira weissfloggi* and *Ditylum brighwellii* are rejected by the model copepod frequently followed by less consumption and this may allow a particular species to bloom despite high copepod abundance (Ryderheim et al. 2022). Such species can be handled for a longer time by the prey and hence, can save the targeted as well as non-targeted species. Similarly, the silica content of the Antarctic bloom-forming species *Fragilariopsis kerguelensis* is usually three folds higher than the

normal diatoms (Smetacek, 1999) and can increase the resistance against grazing and forms dense bloom that sinks efficiently. Diatoms are usually actively grazed by mesozooplankton (medium size) as well as microzooplankton (small size) in the Arabian Sea (Roman et al. 2000). However, the size of the phytoplankton cell plays a key role in trophic transfer as there is a direct connection between the prey and predator body size. For optimal grazing, the ratio between copepod body size and diatom frustule should be 18:1 on average (Hansen et al. 1994) and therefore, the cells above this range may escape grazing and sink. The cells below this ratio can be effectively grazed and may contribute less to the sedimentary organic matter. Large diatoms are highly efficient for sinking and are evident in the contemporary as well as prehistoric oceans (Kemp et al. 2006; Buesseler and Boyd, 2009). Likewise, the higher abundance of large-celled diatoms like *Coscinodiscus* and *Rhizosolenia* in the sediment from the northern stations supports the hypothesis that large frustules escaped grazing and made their way to the sediment as was also noted by Rixen et al. (2019a).

The frustules of the chain-forming small centric diatoms *Thalassiosira* and pennate diatoms like *Fragilaria*, *Pseudo-nitzschia*, and *Nitzschia* dominated the surface sediment from the southern stations that usually remain oligotrophic. In solitary, these species can be grazed due to their smaller cell size, however, their chain formation is likely to help them escape grazing (Bjærke et al. 2015; Lürling, 2021) by increasing the overall surface area which may also accelerate their sinking potential. Moreover, the low DSi level may also promote diatom growth with thinner frustules that can be grazed by copepods. The functioning of the microbial loop in the oligotrophic central Arabian Sea has been reported by an earlier study (Blackford and Burkill, 2002) indicating that the major carbon flow could be via microzooplankton and heterotrophs. The silicious radiolarians preserved in the sediment can be representative of microzooplankton that feed mostly on small phytoplankton, bacteria, and small copepods (Caron et al. 1995). In a previous study, a high abundance of radiolarians was also documented in the central Arabian Sea sediment samples (Gupta, 2003). Our results are consistent with these observations and the higher abundance of radiolarians (Fig. 3F) in the south indicated that microzooplankton grazing (Swanberg and Anderson, 1985) can be stronger due to the dominance of small-sized phytoplankton in the south.

4.3 The presence of OMZ in governing the organic matter export

The central Arabian Sea houses one of the most prominent OMZs between 150-1000 m due to the high surface productivity related to atmospheric forcing and restricted ventilation of the mesopelagic waters (Naqvi, 1990; Banse et al. 2014; Rixen et al. 2020). In the south during the summer monsoon, this OMZ extends to 9 °N, and during the winter monsoon, it moves up to 11 °N (Shenoy et

al. 2020). However, the most intense part is situated towards the northern Arabian Sea (Sarma et al. 2020) and it exists just below the euphotic zone; however, in the south, its vertical expansion narrows down and slowly diminishes southward. Specifically, the secondary nitrite maxima denoting the boundary of OMZ was found to be 250 m thick within 19 -15.5 °N (64 °E), whereas thinned to 50 m at 11 °N (Keil et al. 2016). The presence of OMZ impinging the sediment may facilitate better preservation of organic matter (Keil and Cowie, 1999). However, the OMZ is confined up to 1500 m inside the core area and does not reach the sediment-water interface in the sampling stations where water depth was >3200 m with gradually increasing dissolved oxygen levels downwards. This can dismiss the possibility of higher organic carbon accumulation due to OMZ in the sediment-water interface. Nevertheless, the presence of OMZ in the intermediate water depth may impact the particle flux during the sinking (Keil et al. 2016). A fraction of phytodetritus generated in the euphotic zone undergoes trophic transfer and the rest eventually sinks. However, a substantial portion of the sinking particles ($\approx 70\%$ of organic matter) gets lost (particle flux attenuation) due to heterotrophic respiration within the twilight zone (50 -1000 m) (Suess, 1980) before reaching the bathypelagic. This process is directly controlled by the presence of oxygen and microbial activity (Giering et al. 2015; Cavan et al. 2017). In the warm water column of the low latitude seas, the flux attenuation can be considerably high due to warmer temperatures that increase the rate of heterotrophic respiration (Marsay et al. 2015). However, the mineralization rates of diatom aggregates have been seen to be impacted by increasing temperature without any change in sinking velocity (Iversen and Ploug, 2013). A model study combining the particle flux measurements from the Arabian Sea (Keil et al. 2016) indicated that in the upper mesopelagic, the OMZ microbial respiration is the key factor, whereas, zooplankton grazing and sinking rates were the major cause that influences the particle flux attenuation below mesopelagic. Usually, the most productive oceanic areas are less efficient places for carbon export flux due to fast recycling efficiency (Francois et al. 2002). Conversely, the low productive regions are found to be the places for better carbon transfer to the sediment (Francois et al. 2002). The trend observed in this study contradicts this view. However, the higher TOC (Fig. 2B), as well as large diatom abundance (Fig. 2D) on the sediment from the north, may not be driven alone by diatom cell size but could be largely influenced by the presence of the intense OMZ. Within the OMZ (O_2 level $< 5 \mu\text{mol kg}^{-1}$), organic matter degradation can be considerably slower allowing a higher amount of organic matter to be transported to the sediment (Ma et al. 2021). Several other studies have noticed lower particle flux attenuation in oxygen-deficient waters (Martin et al. 1987; Devol and Hartnett, 2001; Keil et al. 2016; Engel et al. 2017; Ma et al. 2021). In the tropical western Pacific, it was noticed that within the OMZ the mineralization rate of sinking POC was slower than the oxic waters (Ma et al. 2021). During the

JGOFS study, Haake et al. (1992) noticed that the presence of OMZ facilitated lower particle export flux attenuation in the Arabian Sea. Similarly, in the Arabian Sea Keil et al. (2016) noticed inhibited dissolved inorganic carbon production by heterotrophic bacterial community within the OMZ compared to the non-OMZ, and the carbon export flux was directly impacted by the strength of the OMZ. The authors have used floating sediment traps in the central Arabian Sea in a transect that covers some of our sampling locations at the end of the monsoon when maximum particle flux can be expected. It was noticed that the flux attenuation at 19-15.5 °N was significantly lower than observed at 11 °N. We also noticed higher organic matter as well as larger and higher numbers of diatoms at the sediments from 21 -15 °N. And lower particle flux at 11 °N is also consistent with our observation. Besides, the stability of diatom frustules depends on their size and thickness and not all frustules can be preserved equally. Frustules build resistance against dissolution by forming an organic matrix (Lewin 1961) that can be degraded by microbial activity leading to dissolution (Bidle and Azam 1999; Roubeix et al. 2008). While getting transported through the OMZ better preservation of frustules can be expected compared to the oxygenated waters, and similarly, our observation also indicates that larger diatoms were able to sink to the sediment before they got remineralized.

Zooplankton grazing not only drives the trophic transfer pathway of organic matter but also fragments particles facilitating further bacterial mineralization and flux attenuation (Briggs et al. 2020). Usually, in the well-oxygenated mesopelagic waters zooplankton graze actively and take part in particle fragmentation by vertical migration. On the other hand, in the case of OMZ, zooplankton standing stock can be considerably lower as their abundance covaries with oxygen levels, and only some particular groups of zooplankton are well adapted to live under such low oxygen levels (Wishner et al. 2018). Wishner et al. (1998) reported a considerable decrease in zooplankton abundance within the OMZ of the Arabian Sea with a clear peak in the upper (200 m) as well as in the lower boundary (600 m) of the OMZ. A similar trend was also noticed in the OMZ of the north Pacific (Wishner et al. 1995). Cavan et al. (2017) showed that a low abundance of zooplankton and consequent reduction of particle fragmentation within the OMZ may directly facilitate particle export flux. This should be mentioned here that the depth of the water column in the northern stations was close to 3500 m which is nearly 700 m less than the southern stations. This indicates that the phytodetritus sinking from the surface may take a slightly longer time to reach the seabed in the southern stations. Furthermore, the smaller cells may sink slower than the larger cells (Buesseler and Boyd, 2009), and the presence of well-oxygenated waters, as well as zooplankton abundance, may further increase the flux attenuation in this region (Cavan et al. 2017). Therefore in the northern stations, a higher abundance of large diatom frustules, as well as higher organic carbon contents, could be because of less grazing and high particle export to the sediment due to the overlying OMZ. Fig. 5 represents a schematic showing the

possible related factors that are responsible for north-south variability in diatom frustule export to the sediment. Diatom-rich phytodetritus flux to the north and the reverse in the south may directly impact benthic biota (Smith et al. 2008; Sweetman et al. 2017). It was observed that some benthic communities prefer to feed on diatom-dominated detritus compared to the organic matter produced by other phytoplankton (Nomaki et al. 2021). Based on the findings of the present study, a different benthic community in the north and south of the central Arabian Sea can be expected and needs to be addressed in the future. Furthermore, phytoplankton biomarker analysis using the same core samples may also provide more insights into the contribution of different phytoplankton groups to phytodetritus flux to the sediment.

Conclusions

- This is the first report on diatom frustule abundance from the abyss of the central Arabian Sea; a high spatial variability was observed in the diversity, abundance, size of diatom frustules from north to south, and such a trend was mostly related to atmospheric forcings, hydrography as well as the presence of the OMZ along the transect.
- Interestingly, the diatom frustule composition from the surface sediment did not reveal a high level of similarity with the community reported from the euphotic zones suggesting that only some diatom frustules that could avoid grazing, microbial degradation, and dissolution during the transport make their way to the sediments.
- In the north, physical forcing driven natural nutrient enrichment events (open ocean upwelling and winter convection) support larger diatoms growth that may escape grazing followed by rapid sinking to the sediment floor due to higher ballasting effect; moreover, the presence of the thick OMZ at intermediate depth in this region could slow down the heterotrophic mineralization process and grazing during the transport and thus might facilitate higher phytodetritus flux to the seafloor.
- Contrarily, in the south, the low nutrient conditions mostly support small and medium-sized diatoms that form chains, and the weak OMZ may accelerate the heterotrophic mineralization rates during the transport of phytodetritus to the seabed.
- Based on the present observations, likely that the north-south variability in diatom-rich phytodetritus flux to the sediment floor may influence the benthic biota as this is their food source and needs further investigation.

Acknowledgments: We are grateful to the Director, CSIR NIO, for his support and encouragement. We are also thankful to the captain, scientists, technical staff, ship cell staff, crew members, deckhands, and the students onboard RV Sindhu Sadhna (SSD 068). We also acknowledge the help of Ms. Teja Naik for her help regarding elemental analysis and Coulometer under the CAF of CSIR NIO. The contribution number is XXXX. This study was conducted under the Council of Scientific and Industrial Research (CSIR) funded program “Impact of Climate Change on the Physics, Biogeochemistry, and the Ecology of the North Indian Ocean (CliCNIO)” (MLP 1802).

Competing interest: This study was conducted in the absence of any financial interest and the authors have no conflict of interest to declare.

Availability of data and materials: All data used in this study are given in the manuscript file and can be available on request.

Authors' contribution: Medhavi Pandey has contributed to field campaigns, sample collection, formal analyses, data analysis, manuscript writing, and reviewing. Haimanti Biswas secured funding and assisted in sample collection, data interpretation, manuscript reviewing, and editing. Mintu Chowdhury helped in sampling and reviewing the manuscript.

Funding: Medhavi Pandey and Mintu Chowdhury were funded by the Department of Science and Technology (DST)- Inspire program and the CSIR.

Declaration: All authors have read, understood, and have complied as applicable with the statement on "Ethical responsibilities of Authors" as found in the Instructions for Authors

References

1. Abrantes, F., Cermeno, P., Lopes, C., Romero, O., Matos, L., Van Iperen, J., Rufino, M. & Magalhães, V. (2016). Diatoms Si uptake capacity drives carbon export in coastal upwelling systems. *Biogeosciences*, 13(14), 4099-4109. <https://doi.org/10.5194/bg-13-4099-2016>
2. Abrantes, F.F.G. & Sancetta, C. (1985). Diatom assemblages in surface sediments reflect coastal upwelling off southern Portugal. *Oceanologica acta*, 8(1), 7-12.
3. Agustí, S., González-Gordillo, J.I., Vaqué, D., Estrada, M., Cerezo, M.I., Salazar, G., Gasol, J.M. & Duarte, C.M. (2015). Ubiquitous healthy diatoms in the deep sea confirm deep carbon injection by the biological pump. *Nature communications*, 6(1),1-8. <https://doi.org/10.1038/ncomms8608>

4. Alonso-González, I.J., Arístegui, J., Lee, C., Sanchez-Vidal, A., Calafat, A., Fabrés, J., Sangrá, P., Masqué, P., Hernández-Guerra, A. & Benítez-Barrios, V. (2010). Role of slowly settling particles in the ocean carbon cycle. *Geophysical research letters*, 37(13). <https://doi.org/10.1029/2010GL043827>
5. Andruleit, H.A., Von Rad, U., Brans, A. & Ittekkot, V. (2000). Coccolithophore fluxes from sediment traps in the northeastern Arabian Sea off Pakistan. *Marine Micropaleontology*, 38(3-4), 285-308. [https://doi.org/10.1016/S0377-8398\(00\)00007-4](https://doi.org/10.1016/S0377-8398(00)00007-4)
6. Anju, M., Sreeush, M.G., Valsala, V., Smitha, B.R., Hamza, F., Bharathi, G. & Naidu, C.V. (2020). Understanding the role of nutrient limitation on plankton biomass over Arabian Sea via 1-D coupled biogeochemical model and bio-Argo observations. *Journal of Geophysical Research: Oceans*, 125(6), e2019JC015502. <https://doi.org/10.1029/2019JC015502>
7. Armbrrecht, L.H., Lowe, V., Escutia, C., Iwai, M., McKay, R. & Armand, L.K. (2018). Variability in diatom and silicoflagellate assemblages during mid-Pliocene glacial-interglacial cycles determined in Hole U1361A of IODP Expedition 318, Antarctic Wilkes Land Margin. *Marine Micropaleontology*, 139, 28-41. <https://doi.org/10.1016/j.marmicro.2017.10.008>
8. Banse, K. & McClain, C.R. (1986). Winter blooms of phytoplankton in the Arabian Sea as observed by the Coastal Zone Color Scanner. *Marine Ecology Progress Series*, 201-211.
9. Banse, K. (1987). Seasonality of phytoplankton chlorophyll in the central and northern Arabian Sea. *Deep Sea Research Part A. Oceanographic Research Papers*, 34(5-6), 713-723. [https://doi.org/10.1016/0198-0149\(87\)90032-X](https://doi.org/10.1016/0198-0149(87)90032-X)
10. Banse, K., Naqvi, S.W.A., Narvekar, P.V., Postel, J.R. & Jayakumar, D.A. (2014). Oxygen minimum zone of the open Arabian Sea: variability of oxygen and nitrite from daily to decadal timescales. *Biogeosciences*, 11(8), 2237-2261. <https://doi.org/10.5194/bg-11-2237-2014>
11. Bauer, S., Hitchcock, G.L. & Olson, D.B. (1991). Influence of monsoonally-forced Ekman dynamics upon surface layer depth and plankton biomass distribution in the Arabian Sea. *Deep Sea Research Part A. Oceanographic Research Papers*, 38(5), 531-553. [https://doi.org/10.1016/0198-0149\(91\)90062-K](https://doi.org/10.1016/0198-0149(91)90062-K)
12. Behrenfeld, M.J., O'malley, R.T., Siegel, D.A., McClain, C.R., Sarmiento, J.L., Feldman, G.C., Milligan, A.J., Falkowski, P.G., Letelier, R.M. & Boss, E.S. (2006). Climate-driven trends in contemporary ocean productivity. *Nature*, 444(7120), 752-755. <https://doi.org/10.1038/nature05317>

13. Bhaskar, P.V., Cardozo, E., Giriyan, A., Garg, A. & Bhosle, N.B. (2000). Sedimentation of particulate matter in the Dona Paula Bay, west coast of India during November to May 1995–1997. *Estuaries*, 23(5), 722-734. <https://doi.org/10.2307/1352898>
14. Bhattathiri, P.M.A., Pant, A., Sawant, S.S., Gauns, M., Matondkar, S.G.P. & Mahanraju, R. (1996). Phytoplankton production and chlorophyll distribution in the eastern and central Arabian Sea in 1994-1995.
1. Bidle, K.D., & Azam, F. (1999). Accelerated dissolution of diatom silica by marine bacterial assemblages. *Nature*, 397(6719), 508-512. <https://doi.org/10.1038/17351>
15. Bjærke, O., Jonsson, P.R., Alam, A. & Selander, E. (2015). Is chain length in phytoplankton regulated to evade predation?. *Journal of Plankton Research*, 37(6), 1110-1119. <https://doi.org/10.1093/plankt/fbv076>
16. Blackford, J.C. & Burkill, P.H. (2002). Planktonic community structure and carbon cycling in the Arabian Sea as a result of monsoonal forcing: the application of a generic model. *Journal of Marine Systems*, 36(3-4), 239-267. [https://doi.org/10.1016/S0924-7963\(02\)00182-3](https://doi.org/10.1016/S0924-7963(02)00182-3)
17. Briggs, N., Dall'olmo, G. & Claustre, H. (2020). Major role of particle fragmentation in regulating biological sequestration of CO₂ by the oceans. *Science*, 367(6479), 791-793. <https://doi.org/10.1126/science.aay1790>
18. Brink, K., Arnone, R., Coble, P., Flagg, C., Jones, B., Kindle, J., Lee, C., Phinney, D., Wood, M., Yentsch, C. & Young, D. (1998). Monsoons boost biological productivity in Arabian Sea. *Eos, Transactions American Geophysical Union*, 79(13), 165-169. <https://doi.org/10.1029/98EO00120>
19. Brock, J.C. & McClain, C.R. (1992). Interannual variability in phytoplankton blooms observed in the northwestern Arabian Sea during the southwest monsoon. *Journal of Geophysical Research: Oceans*, 97(C1), 733-750. <https://doi.org/10.1029/91JC02225>
20. Buesseler, K.O. & Boyd, P.W. (2009). Shedding light on processes that control particle export and flux attenuation in the twilight zone of the open ocean. *Limnology and Oceanography*, 54(4), 1210-1232. <https://doi.org/10.4319/lo.2009.54.4.1210>
21. Buesseler, K.O. (1998). The decoupling of production and particulate export in the surface ocean. *Global Biogeochemical Cycles*, 12(2), 297-310. <https://doi.org/10.1029/97GB03366>
22. Cabrera-Brufau, M., Arin, L., Sala, M.M., Cermeño, P. & Marrasé, C. (2021). Diatom dominance enhances resistance of phytoplanktonic POM to mesopelagic microbial decomposition. *Frontiers in Marine Science*, 8, 754. <https://doi.org/10.3389/fmars.2021.683354>

23. Caron, D.A., Michaels, A.F., Swanberg, N.R. & Howse, F.A. (1995). Primary productivity by symbiont-bearing planktonic sarcodines (Acantharia, Radiolaria, Foraminifera) in surface waters near Bermuda. *Journal of Plankton Research*, 17(1), 103-129. <https://doi.org/10.1093/plankt/17.1.103>
24. Cavan, E.L., Trimmer, M., Shelley, F. & Sanders, R. (2017). Remineralization of particulate organic carbon in an ocean oxygen minimum zone. *Nature Communications*, 8(1), 1-9. <https://doi.org/10.1038/ncomms14847>
25. Chndrasekhararao, A.V., Kurian, S., Vidya, P.J., Gauns, M., Shenoy, D.M., Mulla, A., Naik, H., Reddy, T.V. & Naqvi, S.W.A. (2018). Phytoplankton response to the contrasting physical regimes in the eastern Arabian Sea during north east monsoon. *Journal of Marine Systems*, 182, 56-66. <https://doi.org/10.1016/j.jmarsys.2018.02.002>
26. Chowdhury, M., Biswas, H., Mitra, A., Silori, S., Sharma, D., Bandyopadhyay, D., Shaik, A.U.R., Fernandes, V. & Narvekar, J. (2021). Southwest monsoon-driven changes in the phytoplankton community structure in the central Arabian Sea (2017–2018): After two decades of JGOFS. *Progress in Oceanography*, 197, 102654. <https://doi.org/10.1016/j.pocean.2021.102654>
27. Devol, A.H. & Hartnett, H.E. (2001). Role of the oxygen-deficient zone in transfer of organic carbon to the deep ocean. *Limnology and Oceanography*, 46(7), 1684-1690. <https://doi.org/10.4319/lo.2001.46.7.1684>
28. Du Clos, K.T., Karp-Boss, L. & Gemmell, B.J. (2021). Diatoms rapidly alter sinking behavior in response to changing nutrient concentrations. *Limnology and Oceanography*, 66(3), 892-900. <https://doi.org/10.1002/lno.11649>
29. Engel, A., Wagner, H., Le Moigne, F.A. & Wilson, S.T. (2017). Particle export fluxes to the oxygen minimum zone of the eastern tropical North Atlantic. *Biogeosciences*, 14(7), 1825-1838. <https://doi.org/10.5194/bg-14-1825-2017>
30. Falkowski, P.G., Flagg, C.N., Rowe, G.T., Smith, S.L., Whitedge, T.E. & Wirick, C.D. (1988). The fate of a spring phytoplankton bloom: export or oxidation?. *Continental Shelf Research*, 8(5-7), 457-484. [https://doi.org/10.1016/0278-4343\(88\)90064-7](https://doi.org/10.1016/0278-4343(88)90064-7)
31. Field, C.B., Behrenfeld, M.J., Randerson, J.T. & Falkowski, P. (1998). Primary production of the biosphere: integrating terrestrial and oceanic components. *Science*, 281(5374), 237-240. <https://doi.org/10.1126/science.281.5374.237>
32. Findlater, J. (1971). *Mean monthly airflow at low levels over the western Indian Ocean*. HM Stationery Office.

33. Francois, R., Honjo, S., Krishfield, R. & Manganini, S. (2002). Factors controlling the flux of organic carbon to the bathypelagic zone of the ocean. *Global Biogeochemical Cycles*, 16(4), 34. <https://doi.org/10.1029/2001GB001722>
34. Garrison, D.L., Gowing, M.M. & Hughes, M.P. (1998). Nano-and microplankton in the northern Arabian Sea during the Southwest Monsoon, August–September 1995 A US–JGOFS study. *Deep Sea Research Part II: Topical Studies in Oceanography*, 45(10-11), 2269-2299. [https://doi.org/10.1016/S0967-0645\(98\)00071-X](https://doi.org/10.1016/S0967-0645(98)00071-X)
35. Garrison, D.L., Gowing, M.M., Hughes, M.P., Campbell, L., Caron, D.A., Dennett, M.R., Shalapyonok, A., Olson, R.J., Landry, M.R., Brown, S.L. & Liu, H.B. (2000). Microbial food web structure in the Arabian Sea: a US JGOFS study. *Deep Sea Research Part II: Topical Studies in Oceanography*, 47(7-8), 1387-1422. [https://doi.org/10.1016/S0967-0645\(99\)00148-4](https://doi.org/10.1016/S0967-0645(99)00148-4)
36. Gauns, M., Madhupratap, M., Ramaiah, N., Jyothibabu, R., Fernandes, V., Paul, J.T. & Kumar, S.P. (2005). Comparative accounts of biological productivity characteristics and estimates of carbon fluxes in the Arabian Sea and the Bay of Bengal. *Deep Sea Research Part II: Topical Studies in Oceanography*, 52(14-15), 2003-2017. <https://doi.org/10.1016/j.dsr2.2005.05.009>
37. Giering, S.L., Sanders, R., Lampitt, R.S., Anderson, T.R., Tamburini, C., Boutrif, M., Zubkov, M.V., Marsay, C.M., Henson, S.A., Saw, K. & Cook, K. (2014). Reconciliation of the carbon budget in the ocean's twilight zone. *Nature*, 507(7493), 480-483. <https://doi.org/10.1038/nature13123>
38. Gupta, S.M. (2003). Orbital frequencies in radiolarian assemblages of the central Indian Ocean: implications on the Indian summer monsoon. *Palaeogeography, Palaeoclimatology, Palaeoecology*, 197(1-2), 97-112. [https://doi.org/10.1016/S0031-0182\(03\)00388-2](https://doi.org/10.1016/S0031-0182(03)00388-2)
39. Haake, B., Ittekkot, V., Ramaswamy, V., Nair, R.R. & Honjo, S. (1992). Fluxes of amino acids and hexosamines to the deep Arabian Sea. *Marine Chemistry*, 40(3-4), 291-314. [https://doi.org/10.1016/0304-4203\(92\)90028-9](https://doi.org/10.1016/0304-4203(92)90028-9)
40. Haake, B., Ittekkot, V., Rixen, T., Ramaswamy, V., Nair, R.R. & Curry, W.B. (1993). Seasonality and interannual variability of particle fluxes to the deep Arabian Sea. *Deep Sea Research Part I: Oceanographic Research Papers*, 40(7), 1323-1344. [https://doi.org/10.1016/0967-0637\(93\)90114-I](https://doi.org/10.1016/0967-0637(93)90114-I)
41. Hansen, B., Bjornsen, P.K. & Hansen, P.J. (1994). The size ratio between planktonic predators and their prey. *Limnology and oceanography*, 39(2), 395-403. <https://doi.org/10.4319/lo.1994.39.2.0395>

42. Iversen, M.H. & Ploug, H. (2013). Temperature effects on carbon-specific respiration rate and sinking velocity of diatom aggregates—potential implications for deep ocean export processes. *Biogeosciences*, 10(6), 4073-4085. <https://doi.org/10.5194/bg-10-4073-2013>
43. Jin, X., Gruber, N., Dunne, J.P., Sarmiento, J.L. & Armstrong, R.A. (2006). Diagnosing the contribution of phytoplankton functional groups to the production and export of particulate organic carbon, CaCO₃, and opal from global nutrient and alkalinity distributions. *Global Biogeochemical Cycles*, 20(2). <https://doi.org/10.1029/2005GB002532>
44. Karnan, C., Jyothibabu, R., Arunpandi, N., Albin, K.J., Parthasarathi, S. & Krishnan, S.S. (2020). Response of microplankton size structure to summer stratification, freshwater influx and coastal upwelling in the Southeastern Arabian Sea. *Continental Shelf Research*, 193, 104038. <https://doi.org/10.1016/j.csr.2019.104038>
45. Keil, R.G. & Cowie, G.L. (1999). Organic matter preservation through the oxygen-deficient zone of the NE Arabian Sea as discerned by organic carbon: mineral surface area ratios. *Marine Geology*, 161(1), 13-22. [https://doi.org/10.1016/S0025-3227\(99\)00052-3](https://doi.org/10.1016/S0025-3227(99)00052-3)
46. Keil, R.G., Neibauer, J.A., Biladeau, C., Van Der Elst, K. & Devol, A.H. (2016). A multiproxy approach to understanding the "enhanced" flux of organic matter through the oxygen-deficient waters of the Arabian Sea. *Biogeosciences*, 13(7), 2077-2092. <https://doi.org/10.5194/bg-13-2077-2016>
47. Kemp, A.E.S., Pearce, R.B., Grigorov, I., Rance, J., Lange, C.B., Quilty, P. & Salter, I. (2006). Production of giant marine diatoms and their export at oceanic frontal zones: Implications for Si and C flux from stratified oceans. *Global Biogeochemical Cycles*, 20(4). <https://doi.org/10.1029/2006GB002698>
48. Koizumi, I. (1985). Neogene diatom biostratigraphy of the middle latitude western north Pacific, Deep Sea Drilling Project Leg 86. *Init. Repts. DSDP.*, 86, 269-300.
49. Krause, J.W., Schulz, I.K., Rowe, K.A., Dobbins, W., Winding, M.H., Sejr, M.K., Duarte, C.M. & Agustí, S. (2019). Silicic acid limitation drives bloom termination and potential carbon sequestration in an Arctic bloom. *Scientific Reports*, 9(1), 1-11. <https://doi.org/10.1038/s41598-019-44587-4>
50. Lampitt, R.S. (1985). Evidence for the seasonal deposition of detritus to the deep-sea floor and its subsequent resuspension. *Deep Sea Research Part A. Oceanographic Research Papers*, 32(8), 885-897. [https://doi.org/10.1016/0198-0149\(85\)90034-2](https://doi.org/10.1016/0198-0149(85)90034-2)
51. Le Moigne, F.A. (2019). Pathways of organic carbon downward transport by the oceanic biological carbon pump. *Frontiers in Marine Science*, 6, 634. <https://doi.org/10.3389/fmars.2019.00634>

52. Leblanc, K., Queguiner, B., Diaz, F., Cornet, V., Michel-Rodriguez, M., Durrieu De Madron, X., Bowler, C., Malviya, S., Thyssen, M., Grégori, G. & Rembauville, M. (2018). Nanoplanktonic diatoms are globally overlooked but play a role in spring blooms and carbon export. *Nature Communications*, 9(1), 1-12. <https://doi.org/10.1038/s41467-018-03376-9>
2. Lewin, J.C. (1961). The dissolution of silica from diatom walls. *Geochimica et Cosmochimica Acta*, 21(3-4), 182-198. [https://doi.org/10.1016/S0016-7037\(61\)80054-9](https://doi.org/10.1016/S0016-7037(61)80054-9)
53. Lüring, M. (2021). Grazing resistance in phytoplankton. *Hydrobiologia*, 848(1), 237-249. <https://doi.org/10.1007/s10750-020-04370-3>
54. Ma, J., Song, J., Li, X., Wang, Q., Zhong, G., Yuan, H., Li, N. & Duan, L. (2021). The OMZ and Its Influence on POC in the Tropical Western Pacific Ocean: Based on the Survey in March 2018. *Frontiers in Earth Science*, 9, 492. <https://doi.org/10.3389/feart.2021.632229>
55. Madhupratap, M., Kumar, S.P., Bhattathiri, P.M.A., Kumar, M.D., Raghukumar, S., Nair, K.K.C. & Ramaiah, N. (1996). Mechanism of the biological response to winter cooling in the northeastern Arabian Sea. *Nature*, 384(6609), 549-552. <https://doi.org/10.1038/384549a0>
56. Marañón, E. (2015). Cell size as a key determinant of phytoplankton metabolism and community structure. *Annual review of marine science*, 7, 241-264. <https://doi.org/10.1146/annurev-marine-010814-015955>
57. Marsay, C.M., Sanders, R.J., Henson, S.A., Pabortsava, K., Achterberg, E.P. & Lampitt, R.S. (2015). Attenuation of sinking particulate organic carbon flux through the mesopelagic ocean. *Proceedings of the National Academy of Sciences*, 112(4), 1089-1094. <https://doi.org/10.1073/pnas.1415311112>
58. Martin, J.H., Knauer, G.A., Karl, D.M. & Broenkow, W.W. (1987). VERTEX: carbon cycling in the northeast Pacific. *Deep Sea Research Part A. Oceanographic Research Papers*, 34(2), 267-285. [https://doi.org/10.1016/0198-0149\(87\)90086-0](https://doi.org/10.1016/0198-0149(87)90086-0)
59. Mergulhao, L.P., Mohan, R., Murty, V.S.N., Guptha, M.V.S. & Sinha, D.K. (2006). Coccolithophores from the central Arabian Sea: Sediment trap results. *Journal of earth system science*, 115(4), 415-428. <https://doi.org/10.1007/BF02702870>
60. Mouw, C.B., Barnett, A., Mckinley, G.A., Gloege, L. & Pilcher, D. (2016). Phytoplankton size impact on export flux in the global ocean. *Global Biogeochemical Cycles*, 30(10), 1542-1562. <https://doi.org/10.1002/2015GB005355>
61. Nair, R.R., Ittekkot, V., Manganini, S.J., Ramaswamy, V., Haake, B., Degens, E.T., Desai, B.T. & Honjo, S. (1989). Increased particle flux to the deep ocean related to monsoons. *Nature*, 338(6218), 749-751. <https://doi.org/10.1038/338749a0>

62. Naqvi, S.W.A. (1987). Some aspects of the oxygen-deficient conditions and denitrification in the Arabian Sea. *Journal of Marine research*, 45(4), 1049-1072. <https://doi.org/10.1357/002224087788327118>
63. Naqvi, S.W.A., Noronha, R.J., Somasundar, K. & Gupta, R.S. (1990). Seasonal changes in the denitrification regime of the Arabian Sea. *Deep Sea Research Part A. Oceanographic Research Papers*, 37(4), 593-611. [https://doi.org/10.1016/0198-0149\(90\)90092-A](https://doi.org/10.1016/0198-0149(90)90092-A)
64. Naqvi, W.A. (1991). Geographical extent of denitrification in the Arabian Sea in relation to some physical processes. *Oceanologica Acta*, 14(3), 281-290.
65. Nelson, D.M., Tréguer, P., Brzezinski, M.A., Leynaert, A. & Quéguiner, B. (1995). Production and dissolution of biogenic silica in the ocean: revised global estimates, comparison with regional data and relationship to biogenic sedimentation. *Global biogeochemical cycles*, 9(3), 359-372. <https://doi.org/10.1029/95GB01070>
66. Nomaki, H., Rastelli, E., Alves, A., Suga, H., Ramos, S., Kitahashi, T., Tsuchiya, M., Ogawa, N.O., Matsui, Y., Seike, K. & Miyamoto, N. (2021). Abyssal fauna, benthic microbes, and organic matter quality across a range of trophic conditions in the western Pacific ocean. *Progress in Oceanography*, 195, 102591. <https://doi.org/10.1016/j.pocean.2021.102591>
67. Padmakumar, K.B., Thomas, L.C., Vimalkumar, K.G., Devi, C.A., Maneesh, T.P., Vijayan, A., Gupta, G.V.M. & Sudhakar, M. (2017). Hydrobiological responses of the North Eastern Arabian Sea during late winter and early spring inter-monsoons and the repercussions on open ocean blooms. *Journal of the Marine Biological Association of the United Kingdom*, 97(7), 1467-1478. <https://doi.org/10.1017/S0025315416000795>
68. Parab, S.G., Matondkar, S.P., Gomes, H.D.R. & Goes, J.I. (2006). Monsoon driven changes in phytoplankton populations in the eastern Arabian Sea as revealed by microscopy and HPLC pigment analysis. *Continental Shelf Research*, 26(20), 2538-2558. <https://doi.org/10.1016/j.csr.2006.08.004>
69. Paropkari, A.L., Babu, C.P. & Mascarenhas, A. (1992). A critical evaluation of depositional parameters controlling the variability of organic carbon in Arabian Sea sediments. *Marine Geology*, 107(3), 213-226. [https://doi.org/10.1016/0025-3227\(92\)90168-H](https://doi.org/10.1016/0025-3227(92)90168-H)
70. Pfannkuche, O., Sommer, S. & Kähler, A. (2000). Coupling between phytodetritus deposition and the small-sized benthic biota in the deep Arabian Sea: analyses of biogenic sediment compounds. *Deep Sea Research Part II: Topical Studies in Oceanography*, 47(14), 2805-2833. [https://doi.org/10.1016/S0967-0645\(00\)00050-3](https://doi.org/10.1016/S0967-0645(00)00050-3)
71. Prasannakumar, S., Madhupratap, M., Kumar, M.D., Muraleedharan, P.M., De Souza, S.N., Gauns, M. & Sarma, V.V.S.S. (2001). High biological productivity in the central Arabian Sea

- during the summer monsoon driven by Ekman pumping and lateral advection. *Current Science*, 1633-1638.
72. Prell, W.L., Hutson, W.H., Williams, D.F., Bé, A.W., Geitzenauer, K. & Molfino, B. (1980). Surface circulation of the Indian Ocean during the last glacial maximum, approximately 18,000 yr BP. *Quaternary Research*, 14(3), 309-336. [https://doi.org/10.1016/0033-5894\(80\)90014-9](https://doi.org/10.1016/0033-5894(80)90014-9)
 73. Ragueneau, O., Schultes, S., Bidle, K., Claquin, P. & Moriceau, B. (2006). Si and C interactions in the world ocean: Importance of ecological processes and implications for the role of diatoms in the biological pump. *Global Biogeochemical Cycles*, 20(4). <https://doi.org/10.1029/2006GB002688>
 74. Ramaswamy, V., Nair, R.R., Manganini, S., Haake, B. & Ittekkot, V. (1991). Lithogenic fluxes to the deep Arabian Sea measured by sediment traps. *Deep Sea Research Part A. Oceanographic Research Papers*, 38(2), 169-184. [https://doi.org/10.1016/0198-0149\(91\)90078-T](https://doi.org/10.1016/0198-0149(91)90078-T)
 75. Rixen, T., Cowie, G., Gaye, B., Goes, J., Do Rosário Gomes, H., Hood, R.R., Lachkar, Z., Schmidt, H., Segschneider, J. & Singh, A. (2020). Reviews and syntheses: Present, past, and future of the oxygen minimum zone in the northern Indian Ocean. *Biogeosciences*, 17(23), 6051-6080. <https://doi.org/10.5194/bg-17-6051-2020>
 76. Rixen, T., Gaye, B. & Emeis, K.C. (2019a). The monsoon, carbon fluxes, and the organic carbon pump in the northern Indian Ocean. *Progress in oceanography*, 175, 24-39. <https://doi.org/10.1016/j.pocean.2019.03.001>
 77. Rixen, T., Gaye, B., Emeis, K.C. & Ramaswamy, V. (2019b). The ballast effect of lithogenic matter and its influences on the carbon fluxes in the Indian Ocean. *Biogeosciences*, 16(2), 485-503. *Biogeosciences*, 16, 485–503, 2019. <https://doi.org/10.5194/bg-16-485-2019>
 78. Rixen, T., Guptha, M.V.S. & Ittekkot, V. (2005). Deep ocean fluxes and their link to surface ocean processes and the biological pump. *Progress in Oceanography*, 65(2-4), 240-259. <https://doi.org/10.1016/j.pocean.2005.03.006>
 79. Rixen, T., Haake, B., Ittekkot, V., Guptha, M.V.S., Nair, R.R. & Schlüssel, P. (1996). Coupling between SW monsoon-related surface and deep ocean processes as discerned from continuous particle flux measurements and correlated satellite data. *Journal of Geophysical Research: Oceans*, 101(C12), 28569-28582. <https://doi.org/10.1029/96JC02420>
 80. Roman, M., Smith, S., Wishner, K., Zhang, X. & Gowing, M. (2000). Mesozooplankton production and grazing in the Arabian Sea. *Deep Sea Research Part II: Topical Studies in Oceanography*, 47(7-8), 1423-1450. [https://doi.org/10.1016/S0967-0645\(99\)00149-6](https://doi.org/10.1016/S0967-0645(99)00149-6)

81. Roubex, V., Becquevort, S. & Lancelot, C. (2008). Influence of bacteria and salinity on diatom biogenic silica dissolution in estuarine systems. *Biogeochemistry*, 88(1), 47-62. <https://doi.org/10.1007/s10533-008-9193-8>
82. Ryderheim, F., Grønning, J. & Kiørboe, T. (2022). Thicker shells reduce copepod grazing on diatoms. *Limnology and Oceanography Letters*. <https://doi.org/10.1002/lo12.10243>
83. Sarma, V.V.S.S., Bhaskar, T.U., Kumar, J.P. & Chakraborty, K. (2020). Potential mechanisms responsible for occurrence of core oxygen minimum zone in the north-eastern Arabian Sea. *Deep Sea Research Part I: Oceanographic Research Papers*, 165, 103393. <https://doi.org/10.1016/j.dsr.2020.103393>
84. Sawant, S.S. & Madhupratap, M. (1996). Seasonality and composition of phytoplankton in the Arabian Sea.
85. Shenoy, D.M., Suresh, I., Uskaikar, H., Kurian, S., Vidya, P.J., Shirodkar, G., Gauns, M.U. & Naqvi, S.W.A. (2020). Variability of dissolved oxygen in the Arabian Sea Oxygen Minimum Zone and its driving mechanisms. *Journal of Marine Systems*, 204, 103310. <https://doi.org/10.1016/j.jmarsys.2020.103310>
86. Silori, S., Sharma, D., Chowdhury, M., Biswas, H., Cardinal, D. & Mandeng-Yogo, M. (2021). Particulate organic matter dynamics and its isotopic signatures ($\delta^{13}\text{C}_{\text{POC}}$ and $\delta^{15}\text{N}_{\text{PN}}$) in relation to physical forcing in the central Arabian Sea during SW monsoon (2017–2018). *Science of the Total Environment*, 785, 147326. <https://doi.org/10.1016/j.scitotenv.2021.147326>
87. Smetacek, V. (1999). Bacteria and silica cycling. *Nature*, 397(6719), 475-476. <https://doi.org/10.1038/17219>
88. Smetacek, V.S. (1985). Role of sinking in diatom life-history cycles: ecological, evolutionary and geological significance. *Marine biology*, 84(3), 239-251. <https://doi.org/10.1007/BF00392493>
89. Smith, C.R., De Leo, F.C., Bernardino, A.F., Sweetman, A.K. & Arbizu, P.M. (2008). Abyssal food limitation, ecosystem structure and climate change. *Trends in Ecology & Evolution*, 23(9), 518-528. <https://doi.org/10.1016/j.tree.2008.05.002>
90. Smith, C.R., Hoover, D.J., Doan, S.E., Pope, R.H., Demaster, D.J., Dobbs, F.C. & Altabet, M.A. (1996). Phytodetritus at the abyssal seafloor across 10 of latitude in the central equatorial Pacific. *Deep Sea Research Part II: Topical Studies in Oceanography*, 43(4-6), 1309-1338. [https://doi.org/10.1016/0967-0645\(96\)00015-X](https://doi.org/10.1016/0967-0645(96)00015-X)
91. Smith, R.L. & Bottero, J.S. (1977). On upwelling in the Arabian Sea, A voyage of Discovery M. Angel, 291–304.

92. Sridevi, B. & Sarma, V.V.S.S. (2022). Enhanced atmospheric pollutants strengthened winter convective mixing and phytoplankton blooms in the northern Arabian Sea. *Journal of Geophysical Research: Biogeosciences*, e2021JG006527. <https://doi.org/10.1029/2021JG006527>
93. Suess, E. (1980). Particulate organic carbon flux in the oceans—surface productivity and oxygen utilization. *Nature*, 288(5788), 260-263. <https://doi.org/10.1038/288260a0>
94. Suthhof, A., Jennerjahn, T.C., Schäfer, P. & Ittekkot, V. (2000). Nature of organic matter in surface sediments from the Pakistan continental margin and the deep Arabian Sea: amino acids. *Deep Sea Research Part II: Topical Studies in Oceanography*, 47(1-2), 329-351. [https://doi.org/10.1016/S0967-0645\(99\)00109-5](https://doi.org/10.1016/S0967-0645(99)00109-5)
95. Swanberg, N.R. & Anderson, O.R. (1985). The nutrition of radiolarians: Trophic activity of some solitary Spumellaria 1. *Limnology and Oceanography*, 30(3), 646-652. <https://doi.org/10.4319/lo.1985.30.3.0646>
96. Sweetman, A.K., Thurber, A.R., Smith, C.R., Levin, L.A., Mora, C., Wei, C.L., Gooday, A.J., Jones, D.O., Rex, M., Yasuhara, M. & Ingels, J. (2017). Major impacts of climate change on deep-sea benthic ecosystems. *Elementa: Science of the Anthropocene*, 5. <https://doi.org/10.1525/elementa.203>
97. Tarran, G.A., Burkill, P.H., Edwards, E.S. & Woodward, E.M.S. (1999). Phytoplankton community structure in the Arabian Sea during and after the SW monsoon, 1994. *Deep Sea Research Part II: Topical Studies in Oceanography*, 46(3-4), 655-676. [https://doi.org/10.1016/S0967-0645\(98\)00122-2](https://doi.org/10.1016/S0967-0645(98)00122-2)
98. Tomas, C.R. Ed. (1997). *Identifying marine phytoplankton*. Elsevier.
99. Tréguer, P., Bowler, C., Moriceau, B., Dutkiewicz, S., Gehlen, M., Aumont, O., Bittner, L., Dugdale, R., Finkel, Z., Iudicone, D. & Jahn, O. (2018). Influence of diatom diversity on the ocean biological carbon pump. *Nature Geoscience*, 11(1), 27-37. <https://doi.org/10.1038/s41561-017-0028-x>
100. Tréguer, P.J. & De La Rocha, C.L. (2013). The world ocean silica cycle. *Annual review of marine science*, 5, 477-501. <https://doi.org/10.1146/annurev-marine-121211-172346>
101. Volk, T. & Hoffert, M.I. (1985). Ocean carbon pumps: Analysis of relative strengths and efficiencies in ocean-driven atmospheric CO₂ changes. *The carbon cycle and atmospheric CO₂: natural variations Archean to present*, 32, 99-110. <https://doi.org/10.1029/GM032p0099>
102. Wishner, K.F., Ashjian, C.J., Gelfman, C., Gowing, M.M., Kann, L., Levin, L.A., Mullineaux, L.S. & Saltzman, J. (1995). Pelagic and benthic ecology of the lower interface of the Eastern

Tropical Pacific oxygen minimum zone. *Deep Sea Research Part I: Oceanographic Research Papers*, 42(1), 93-115. [https://doi.org/10.1016/0967-0637\(94\)00021-J](https://doi.org/10.1016/0967-0637(94)00021-J)

103. Wishner, K.F., Gowing, M.M. & Gelfman, C. (1998). Mesozooplankton biomass in the upper 1000 m in the Arabian Sea: overall seasonal and geographic patterns, and relationship to oxygen gradients. *Deep Sea Research Part II: Topical Studies in Oceanography*, 45(10-11), 2405-2432. [https://doi.org/10.1016/S0967-0645\(98\)00078-2](https://doi.org/10.1016/S0967-0645(98)00078-2)
104. Wishner, K.F., Seibel, B.A., Roman, C., Deutsch, C., Outram, D., Shaw, C.T., Birk, M.A., Mislan, K.A.S., Adams, T.J., Moore, D. & Riley, S. (2018). Ocean deoxygenation and zooplankton: Very small oxygen differences matter. *Science advances*, 4(12), eaau5180. <https://doi.org/10.1126/sciadv.aau5180>
105. Wyrski, K., Bennett, E.B. & Rochford, D.J. (1971). *Oceanographic atlas of the international Indian Ocean expedition* (Vol. 531). Washington, DC: National Science Foundation.

Figure legends

Figure 1 Map showing sampling locations along the 64 °E, Central Arabian Sea during SSD-068 (Dec 2019). The black dashed line represents the boundary of the Oxygen Minimum Zone (OMZ) demarcated by the 0.5 mmol L⁻¹ O₂ concentration (redrawn from Naqvi, 1991). The white dashed arrow represents the Findlater Jet. The relative contributions of diatom frustules of major species (individual taxa contribution from centric and pennate <2% were summed as “other centric” and “other pennate” respectively) from the surface sediment samples are shown on the right side and the green arrow indicates the size of the major contributing diatom frustule increased northward.

Figure 2 The bubble maps represent the parameters measured in surface sediments: (A) the total inorganic carbon (%) (TIC); (B) the total organic carbon (%) (TOC); (C) the total nitrogen (%) (TN) and (D) the abundance of diatom frustules (valves per g of dry sediment).

Figure 3 (A) Shannon-Wiener diversity index of diatom frustules ($n = 2 \pm SD$); (B) different size classes of diatom frustules; (C) the frustule abundance of centric and pennate diatoms; the frustule abundance of *Coscinodiscus* (D); and (E) *Thalassiosira* of three size ranges; (F) Radiolarian distribution recorded from the surface sediments of northern (21, 19, and 15 °N) and southern (13 and 11 °N) stations. The “*p*” values represent the level of significance (single-factor ANOVA at 95% confidence level) between the northern and the southern stations.

Figure 4 The average relative abundance (%) of the major diatom genera documented from the upper 60 m water column during the summer monsoon in 2017 and 2018 from the north (A) and south (B) (taken from Chowdhury et al. 2021). The lower panel shows the average relative % of major diatom frustules found from the surface sediments of the north (C) and south (D) of the central Arabian Sea in the current study.

Figure 5 Schematic showing how the surface processes are linked to particle flux to the sediment in the central Arabian Sea. In the northern stations, both “open ocean” upwelling during the summer monsoon and convective mixing during the winter monsoon lead to nutrient enrichment and diatom-dominated phytoplankton blooms. On the contrary, the southern stations remain mostly nutrient-poor and small chain-forming diatoms usually dominate. The larger diatoms with thick frustules in the north may escape grazing and sink rapidly due to higher sinking velocity. The presence of intense OMZ towards the north could facilitate higher particle flux to the sediment due to lower zooplankton fragmentation as well as low heterotrophic metabolism. On the other hand, in the south, the smaller diatoms may sink slowly and due to the less intensification of OMZ, zooplankton abundance as higher dissolved oxygen may enhance flux attenuation leading to lower particle flux in the south. This spatial variability in particle flux to the sediment may have important consequences on benthic biota

Supplementary Figure 1 Light microscopic images of some commonly found centric and pennate diatom frustules obtained from the central Arabian Sea surface sediments. *Coscinodiscus* sp. (A-B), *Thalassiosira* sp. (C-D); *Rhizosolenia* sp. (E), *Hemidiscus* sp. (F), *Cyclotella* sp. (G), *Actinoptychus* sp. (H), *Bacillaria* sp. (I), *Fragilariopsis* sp. (J), *Fragilaria* sp. (K), *Navicula* sp. (L), *Pseudo-nitzschia* sp. (M), *Nitzschia* sp. (N-O), Radiolarians (P-S) at scale bar 10 μm.

Table: 1 Parameter analyzed from the surface sediments. Total inorganic carbon = TIC, total organic carbon = TOC, total nitrogen =TN, and selected characterization of diatom frustules. (average \pm SD, N= 2).

Latitude (°N)	TIC (%)	TOC (%)	TN (%)	Diatom Frustules (No. $\times 10^4$ cells g ⁻¹)	Diatom frustules from three size classes (No. $\times 10^4$ cells g ⁻¹)			Centric Diatom (No. $\times 10^4$ cells g ⁻¹)	Pennate Diatom (No. $\times 10^4$ cells g ⁻¹)	<i>Coscinodiscus</i> frustule in sediment (No. $\times 10^4$ cells g ⁻¹)			<i>Thalassiosira</i> frustule in sediment (No. $\times 10^4$ cells g ⁻¹)		
					<30 μ m	30-60 μ m	>60 μ m			<30 μ m	30-60 μ m	>60 μ m	<30 μ m	30-60 μ m	>60 μ m
21	3.15 \pm 0.02	1.03 \pm 0.01	0.11 \pm .002	5.92 \pm .03	0.45 \pm 0.07	2.53 \pm 07	2.94 \pm 17	4.67 \pm 0.07	1.25 \pm 0.10	0.02 \pm 0.00	1.08 \pm 0.14	1.39 \pm 0.04	0.28 \pm 0.03	0.86 \pm 0.14	0.12 \pm 0.06
19	5.57 \pm 0.03	0.93 \pm 0.01	0.09 \pm .002	6.50 \pm .17	0.66 \pm 0.23	3.26 \pm 00	2.58 \pm 06	5.58 \pm 0.06	0.92 \pm 0.00	0.03 \pm 0.04	1.56 \pm 0.23	1.61 \pm 0.01	0.43 \pm 0.13	1.26 \pm 0.25	0.10 \pm 0.00
15	6.53 \pm 0.04	0.94 \pm 0.01	0.07 \pm .006	5.35 \pm .52	0.63 \pm 0.04	3.04 \pm 45	1.68 \pm 03	4.75 \pm 0.35	0.60 \pm 0.17	0.00 \pm 0.00	1.48 \pm 0.31	1.01 \pm 0.01	0.55 \pm 0.01	1.02 \pm 0.00	0.11 \pm 0.01
13	7.51 \pm 0.09	0.74 \pm 0.08	0.06 \pm .007	4.76 \pm .34	0.76 \pm 0.11	2.27 \pm 16	1.73 \pm 06	4.23 \pm 0.33	0.53 \pm 0.01	0.00 \pm 0.00	0.5 \pm 0. 11	1.02 \pm 0.03	0.75 \pm 0.10	1.39 \pm 0.10	0.23 \pm 0.04
11	6.47 \pm 0.16	0.74 \pm 0.11	0.07 \pm .001	3.29 \pm .07	0.44 \pm 0.23	1.52 \pm 35	1.33 \pm 17	2.62 \pm 0.03	0.67 \pm 0.01	0.00 \pm 0.00	0.15 \pm 0.01	0.48 \pm 0.08	0.44 \pm 0.23	1.08 \pm 0.28	0.20 \pm 0.03

Table 2. Individual diatom frustules abundance (valves g⁻¹ dry sediment) and relative abundance (RP %) in the surface sediments from 5 locations in the Central Arabian Sea (average ±SD n = 2).

Diatom Frustules	21 °N		19 °N		15 °N		13 °N		11 °N	
	Valve g ⁻¹	RP (%)	Valve g ⁻¹	RP (%)	Valve g ⁻¹	RP (%)	Valve g ⁻¹	RP (%)	Valve g ⁻¹	RP (%)
<i>Thalassiosira</i> sp.	12600±2263	21.29	17900±1273	27.57	16800±283	31.58	23700±2404	49.74	17200±283	52.30
<i>Coscinodiscus</i> sp.	24900±1838	42.05	32000±2828	49.19	24900±2970	46.49	15200±1414	31.91	6300±990	19.12
<i>Cyclotella</i> sp.	2700±141	4.56	400±0	0.62	300±141	0.58	-	-	-	-
<i>Triceratium</i> sp.	600±283	1.01	400±283	0.62	700±424	1.35	100±141	0.22	-	-
<i>Rhizosolenia</i> sp.	4400±0	7.43	2600±849	4.02	1000±0	1.88	500±141	1.06	900±141	2.74
<i>Hemidiscus</i> sp.	600±0	1.01	1200±283	1.84	2800±1131	5.15	2800±283	5.92	1800±283	5.48
<i>Actinoptychus</i> sp.	500±141	0.84	300±141	0.46	300±141	0.58	-	-	-	-
<i>Proboscia</i> sp.	400±0	0.68	-	-	-	-	-	-	-	-
<i>Leptocylindrus</i> sp.	-	-	1000±0	1.54	700±424	1.28	-	-	-	-
<i>Fragilaria</i> sp.	1100±141	1.86	300±141	0.46	1200±566	2.20	600±849	1.33	1000±0	3.04
<i>Nitzschia</i> sp.	1100±424	1.86	1200±0	1.85	1100±424	2.03	1200±849	2.46	500±424	1.51
<i>Pseudo-nitzschia</i> sp.	2900±707	4.90	3100±141	4.77	2000±0	3.76	2200±849	4.57	3100±141	9.43
<i>Fragilariopsis</i> sp.	100±141	0.17	-	-	300±424	0.52	900±424	1.93	1300±424	3.94
<i>Thalassionema</i> sp.	4300±707	7.26	4300±1273	6.59	1300±424	2.40	300±141	0.64	700±141	2.13
<i>Navicula</i> sp.	400±283	0.68	200±0	0.31	-	-	100±141	0.22	-	-

<i>Bacillaria</i> sp.	1100±424	1.86	-	-	-	-	-	-	-	-
<i>Diploneis</i> sp.	100±141	0.17	-	-	-	-	-	-	-	-
<i>Gyrosigma</i> sp.	200±0	0.34	-	-	-	-	-	-	-	-
<i>Pleurosigma</i> sp.	100±141	0.17	100±141	0.15	-	-	-	-	-	-
<i>Amphiprora</i> sp.	400±282	0.67	-	-	-	-	-	-	-	-
<i>Eunotia</i> sp.	100±141	0.17	-	-	100±141	0.20	-	-	-	-
<i>Epithemia</i> sp.	-	-	-	-	-	-	-	-	100±141	0.31
<i>Lioloma</i> sp.	600±283	1.01	-	-	-	-	-	-	-	-

Supplementary Table 1: Physicochemical parameters noted during the summer monsoons 2017 -2018 taken from Chowdhury et al. (2021) within the upper 60 m water column.

Parameter	NFJ		SFJ	
	2017	2018	2017	2018
Wind speed	8.27±0.41	9.93±0.90	8.82±0.19	9.98±0.54
MLD	56±24	53±13	85±18	128±7.0
Temperature (°C)	26.86±1.13	26.05±0.86	27.32±0.22	26.34±0.35
Salinity (PSU)	36.46±0.10	36.41±0.13	36.41±0.00	36.39±0.09
Dissolved oxygen (ml/l)	4.02±0.76	3.82±0.71	4.45±0.10	4.17±0.06
Nitrate+nitrite (µmol L ⁻¹)	2.39±5.02	5.26±4.35	1.27±0.90	4.05±1.52
Dissolved Inorganic Silicate (µmol L ⁻¹)	1.48±1.35	0.92±1.37	1.49±0.21	2.92±0.96
Dissolved inorganic phosphate (µmol L ⁻¹)	0.69±0.43	0.84±0.51	0.35±0.11	0.84±0.11
Cell abundance (no x10 ³ L ⁻¹)	2.59±2.49	20.80±21.11	0.65±0.49	7.68±3.06
Diatom:dinoflagellates	8.27±6.08	4.09±2.20	1.56±1.85	1.36±1.05
Centric:Pennate	64.86±40.9	10.57±22.63	10.05±27.11	0.98±0.81
Diversity	1.43±0.6	2.24±0.45	1.87±0.49	2.34±0.27

Supplementary Table: 2 The major diatom species reported in earlier studies from the water column in the central Arabian Sea during both summer and winter monsoons. Please note that the station locations are chosen close to the present study area.

Source	Sampling Period	Location	Parameter studied	Major diatom species found
Winter monsoon				
Parab et al. 2006	2003	19 °N, 66.8 °E; 20.4 °N, 66 °E; 21 °N, 67 °E	Phytoplankton community and pigment analysis	Diatom dominated community; reported <i>Coscinodiscus nitidus</i> , <i>Chaetoceros curvisetus</i> , <i>Nitzschia closterium</i> , <i>Lioloma pacificus</i> , <i>Nitzschia sigma</i> , <i>Diploneis rectangulata</i> , <i>Cocconeis scutellum</i> , <i>Planktoniella sol</i> , and <i>Navicula macunosa</i>
Padmakumar et al. 2017	2009, 2011 and 2012	22 °N, 65.5 °E; 21 °N 66 °E	Phytoplankton community	Diatoms reported <i>Rhizosolenia hebetata</i> , <i>Rhizosolenia</i> sp., <i>Chaetoceros lorenzianus</i> , <i>Guinardia striata</i> , <i>Thalassiosira</i> sp., <i>Haslea</i> sp., <i>Cylindrotheca closterium</i> , <i>Pseudo-nitzschia</i> sp., etc.
Chndrasekhararao et al. 2018	2015 and 2017	21 °N to 9 °N (each degree interval) along 68 °E	Pigment analysis and flow cytometer	North (~21 °N) dominated by larger diatoms; south of ~16 °N favoured Pico plankton (<i>Prochlorococcus</i> and <i>Synechococcus</i>) and Nano plankton.
Summer monsoon				
Sawant and Madhupratap. Indian-JGOFS	1994-1995	11 °N, 64 °E	Phytoplankton community	<i>Nitzschia longissima</i> , <i>N. seriata</i> , <i>Rhizosolenia</i> sp., <i>Chaetoceros</i> sp.
Garrison et al. 1998, Garrison et al. 2000 US-JGOFS	1995	15.08 °N, 63.48 °E (S9); 14.25 °N, 64.95 °E	Autotrophic and heterotrophic nano-and microplankton	S9- <i>Rhizosolenia</i> sp., <i>Haslea gigantea</i> , other pennates, <i>Phaeocystis</i> sp., S11- <i>Rhizosolenia</i> sp., <i>Phaeocystis</i> sp.,

		(S11); 11.95 °N, 64.95 °E (S13); 10.70 °N, 64.95 °E (S14); 9.90 °N, 64.95 °E (S15)	from Oman coast to central AS (Southern transect only)	<i>Thalassiothrix</i> sp., S13 and S15- Picoplankton dominated
Tarran et al. 1999	1994	14.05 °N, 63.26 °E (A4); 12.04 °N, 64.47 °E (A5); 10.23 °N, 65.54 °E (A6)	Diatoms, dinoflagellates, coccolithophores, nanoflagellates, picophytoplankton and prokaryote algae	<i>Synechococcus</i> spp. dominated all stations; large sized diatoms dominated the coastal upwelled waters; <i>Prochlorophytes</i> dominated the oligotrophic stratified waters
Gauns et al. 2005 Indian-JGOFS	1994-1995	11, 15 and 19 °N along 64 °E	Phytoplankton and zooplankton community and carbon flux	High flux obtained for summer as well as winter monsoon
Chowdhury et al. 2021	2017, 2018	21 to 11 °N (each degree interval) along 64 °E	Phytoplankton community, Zooplankton collection, and biomass estimation	North (21–20 °N): large centric diatoms (<i>Rhizosolenia imbricata</i> , <i>R. hebetata</i> and <i>Coscinodiscus</i> <i>radiatus</i>) and in south (11–15 °N) small pennate diatoms (<i>Pseudo-</i> <i>nitzschia</i> , <i>Navicula</i> , <i>Nitzschia</i>) dominated.

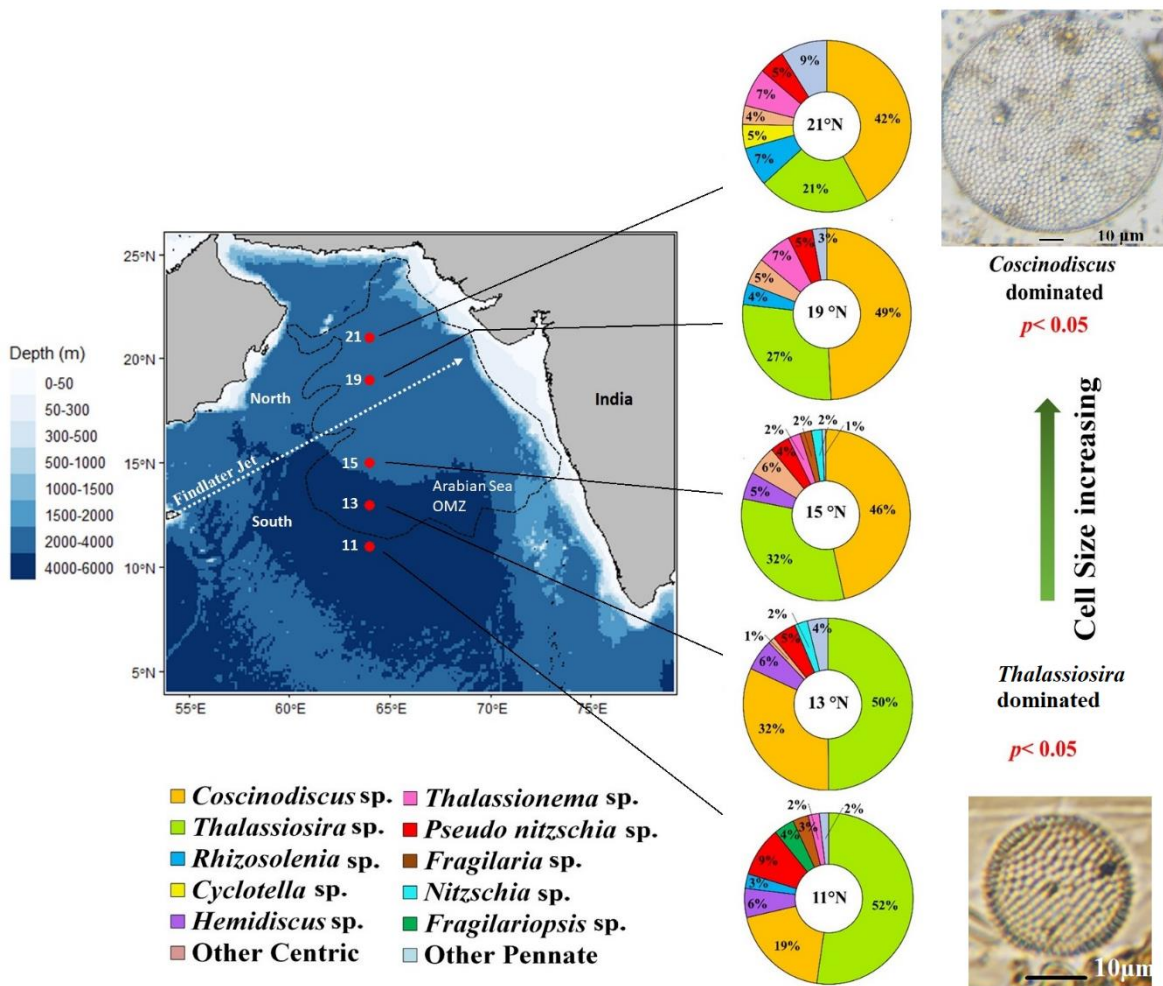


Figure 1 Map showing sampling locations along the 64°E, Central Arabian Sea during SSD-068 (Dec 2019). The black dashed line represents the boundary of the Oxygen Minimum Zone (OMZ) demarcated by the 0.5 mmol L⁻¹ O₂ concentration (redrawn from Naqvi, 1991). The white dashed arrow represents the Findlater Jet. The relative contributions of diatom frustules of major species (individual taxa contribution from centric and pennate <2% were summed as “other centric” and “other pennate” respectively) from the surface sediment samples are shown on the right side and the green arrow indicates the size of the major contributing diatom frustule increased northward.

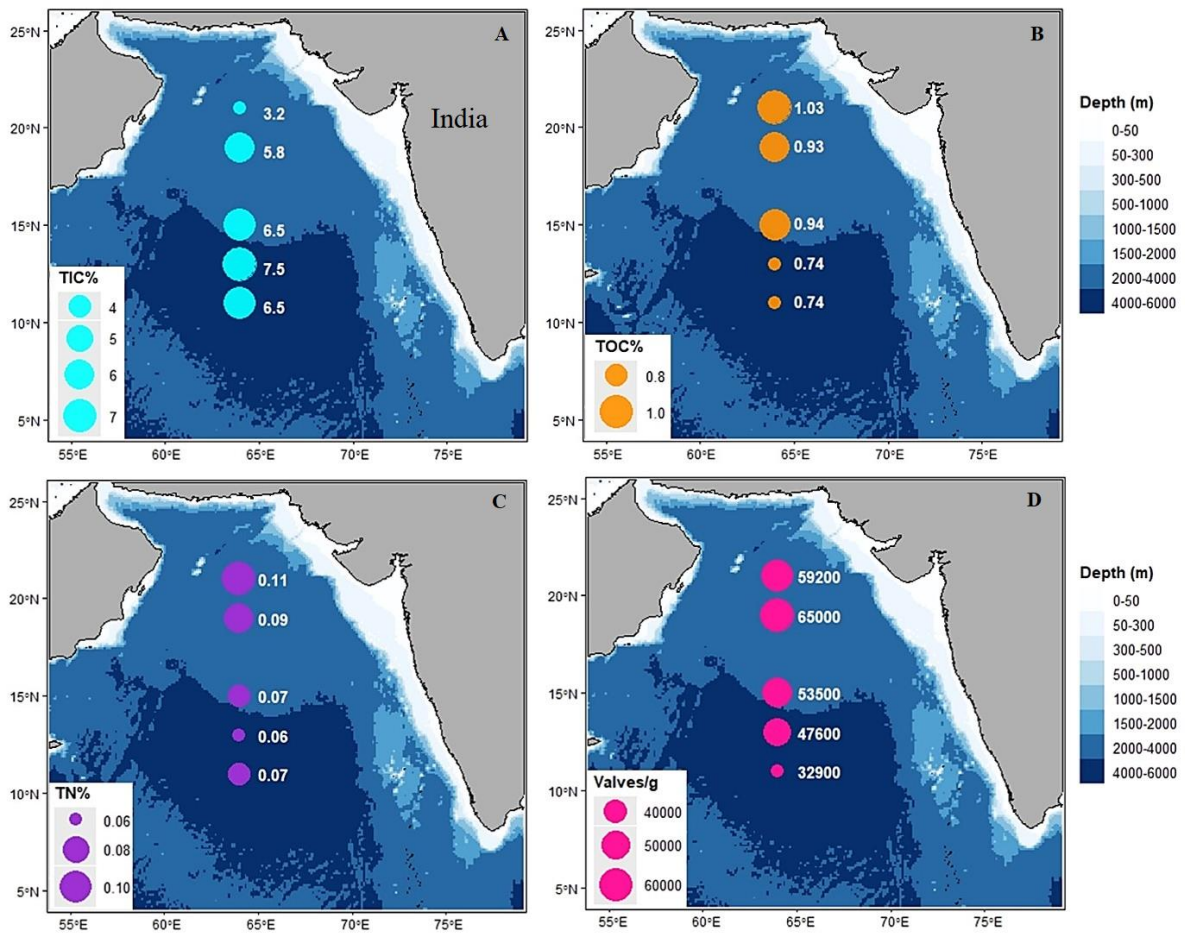


Figure 2 The bubble maps represent the parameters measured in surface sediments: (A) the total inorganic carbon (%) (TIC); (B) the total organic carbon (%) (TOC); (C) the total nitrogen (%) (TN) and (D) the abundance of diatom frustules (valves per g of dry sediment).

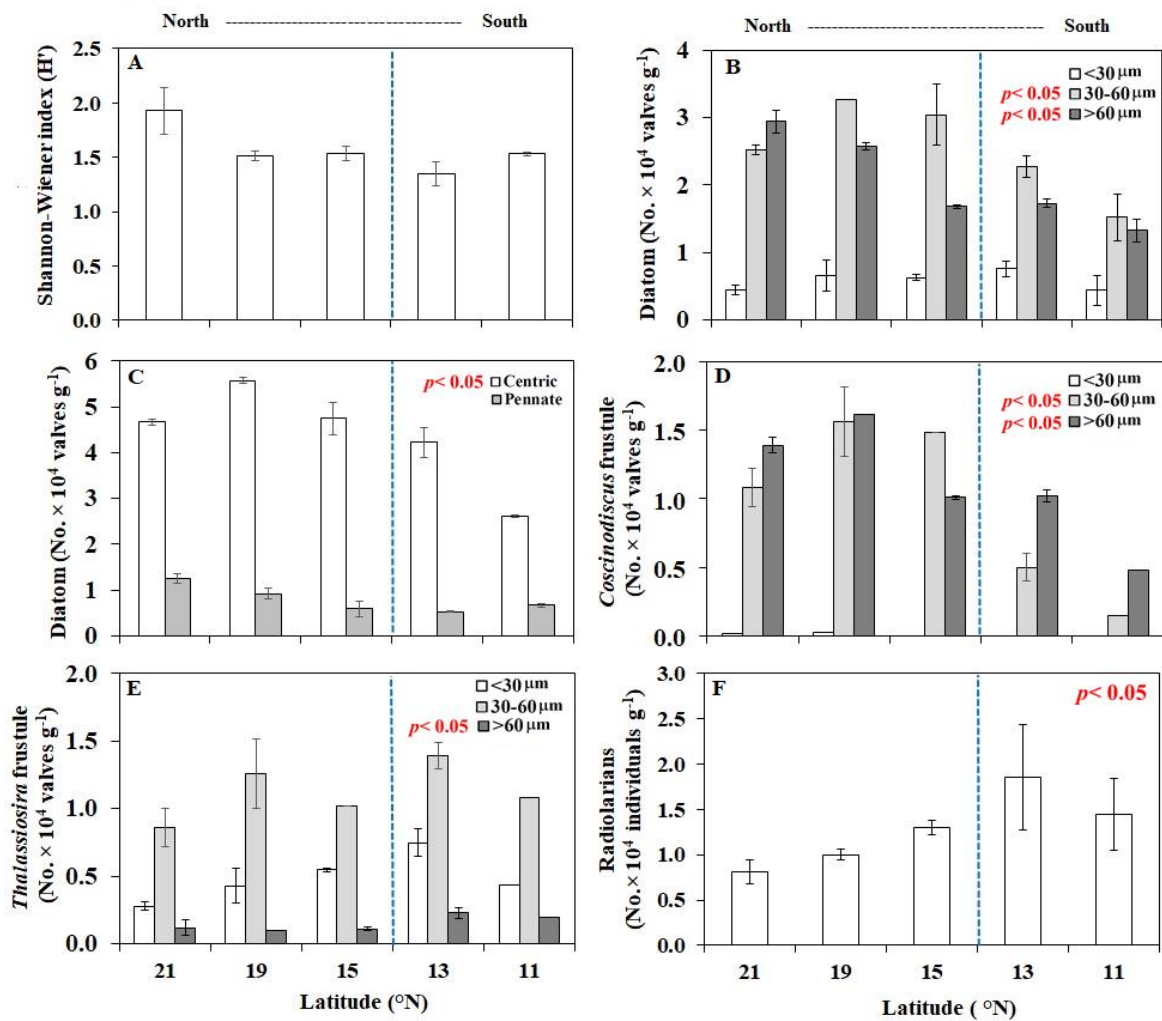
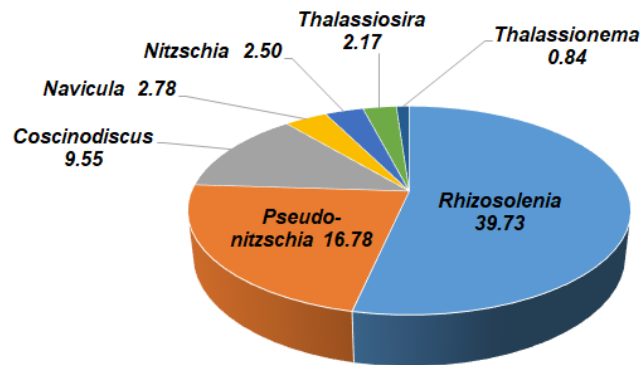
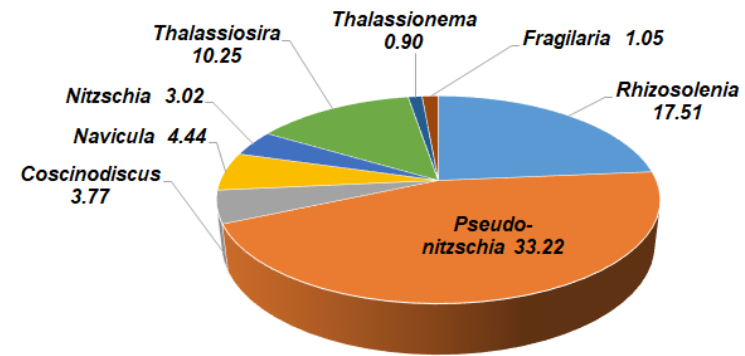


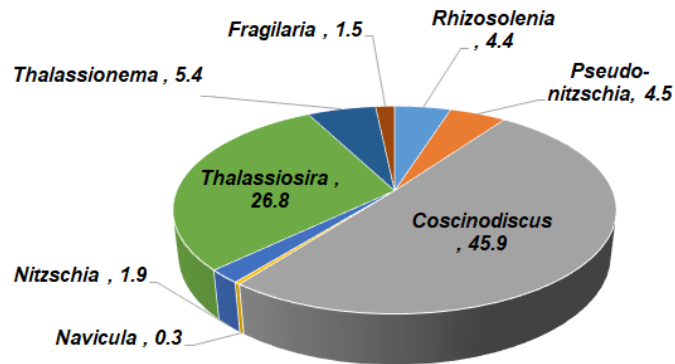
Figure 3 (A) Shannon-Wiener diversity index of diatom frustules ($n = 2 \pm SD$); (B) different size classes of diatom frustules; (C) the frustule abundance of centric and pennate diatoms; the frustule abundance of *Coscinodiscus* (D); and (E) *Thalassiosira* of three size ranges; (F) Radiolarian distribution recorded from the surface sediments of northern (21, 19, and 15 °N) and southern (13 and 11 °N) stations. The “ p ” values represent the level of significance (single-factor ANOVA at 95% confidence level) between the northern and the southern stations.



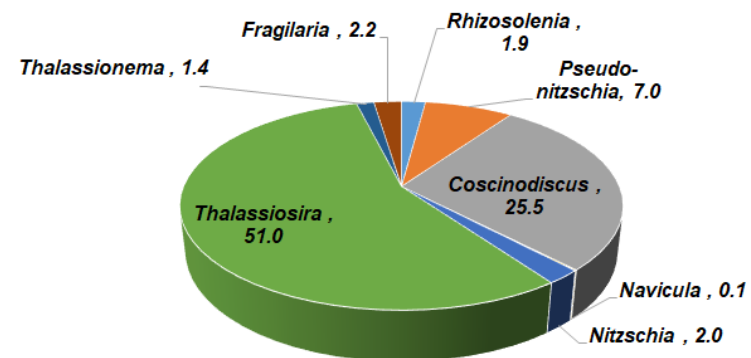
A. North (Water Column)



B. South (Water Column)

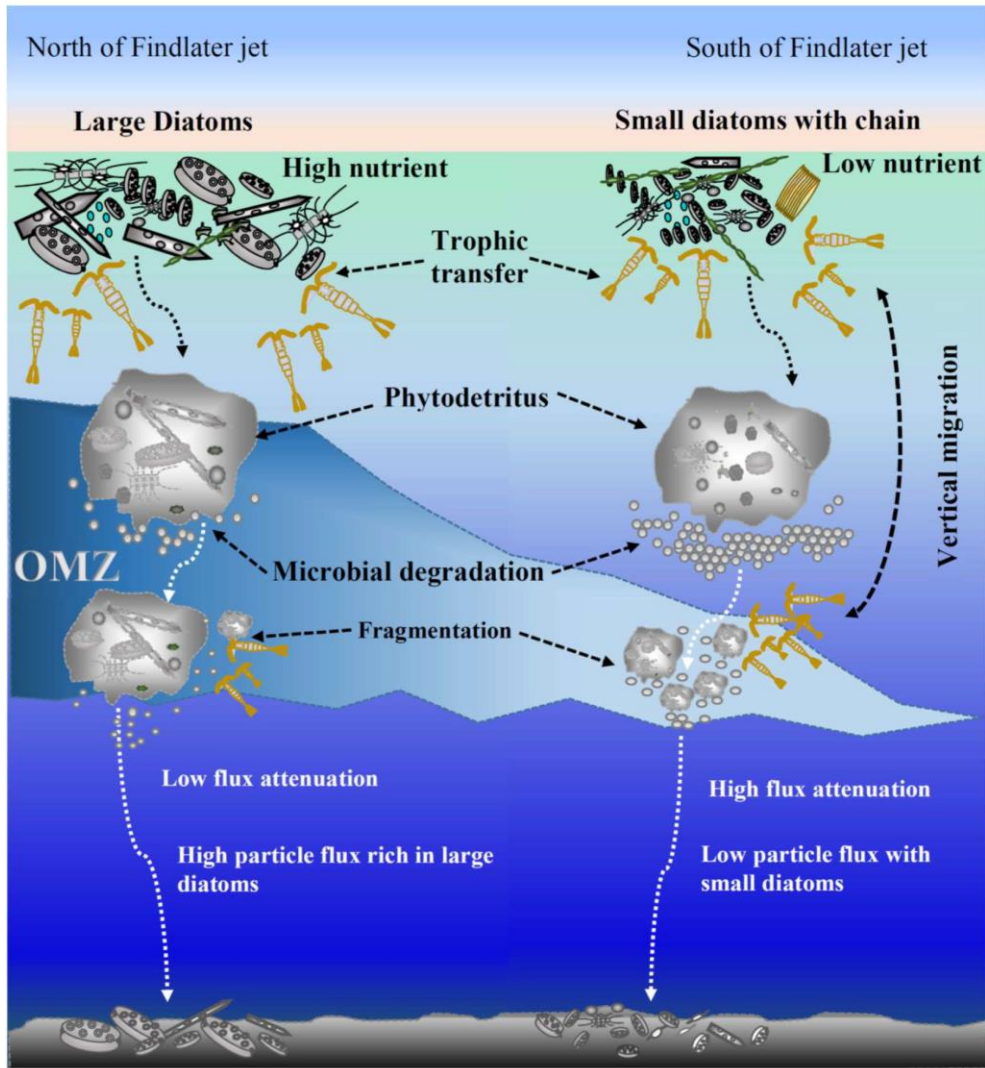


C. North (Surface Sediment)



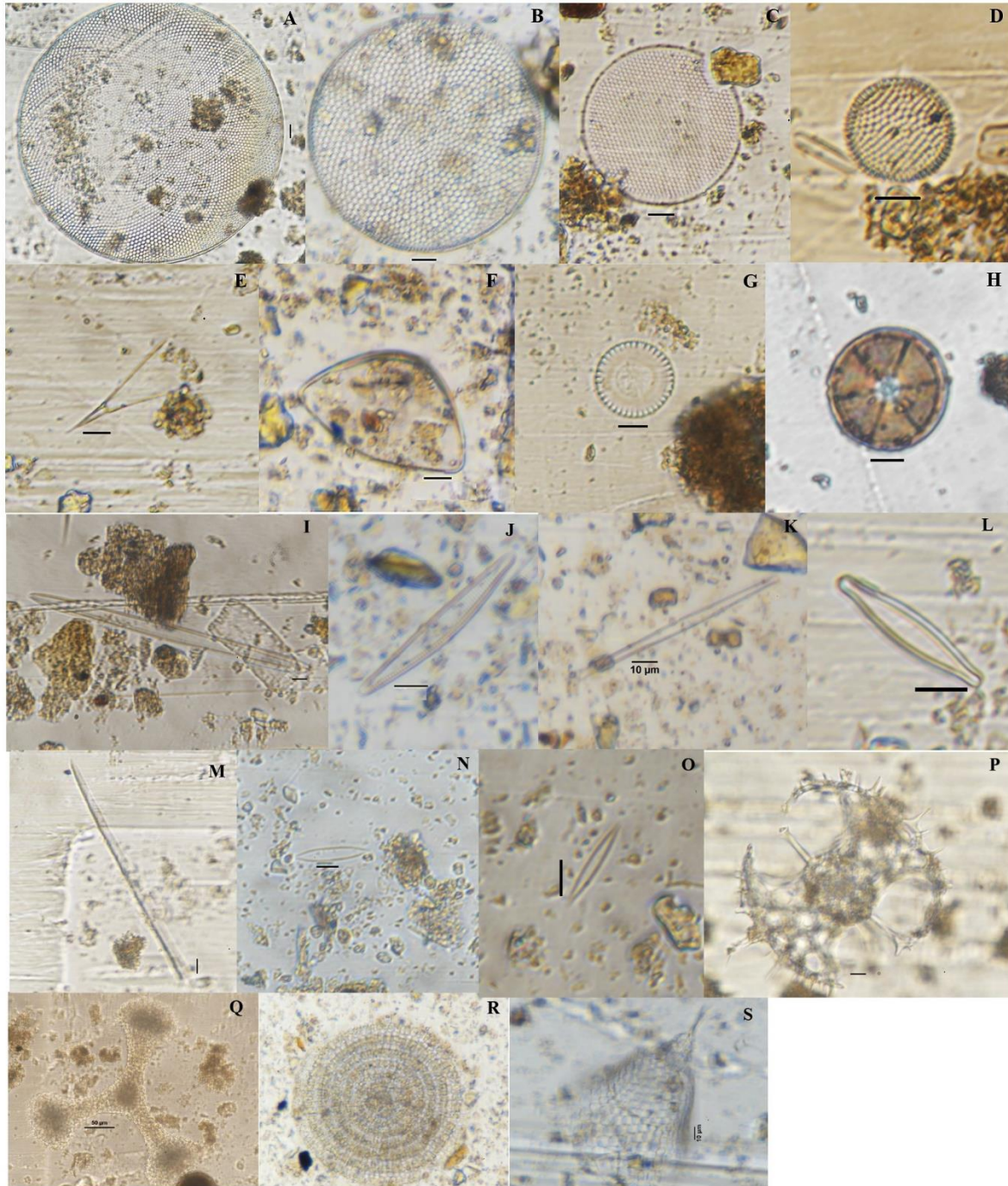
D. South (Surface Sediment)

Figure 4 The average relative abundance (%) of the major diatom genera documented from the upper 60 m water column during the summer monsoon in 2017 and 2018 from the north (A) and south (B) (taken from Chowdhury et al. 2021). The lower panel shows the average relative % of major diatom frustules found from the surface sediments of the north (C) and south (D) of the central Arabian Sea in the current study.



*Not to scale

Figure 5 Schematic showing how the surface processes are linked to particle flux to the sediment in the central Arabian Sea. In the northern stations, both “open ocean” upwelling during the summer monsoon and convective mixing during the winter monsoon lead to nutrient enrichment and diatom-dominated phytoplankton blooms. On the contrary, the southern stations remain mostly nutrient-poor and small chain-forming diatoms usually dominate. The larger diatoms with thick frustules in the north may escape grazing and sink rapidly due to higher sinking velocity. The presence of intense OMZ towards the north could facilitate higher particle flux to the sediment due to lower zooplankton fragmentation as well as low heterotrophic metabolism. On the other hand, in the south, the smaller diatoms may sink slowly and due to the less intensification of OMZ, zooplankton abundance as higher dissolved oxygen may enhance flux attenuation leading to lower particle flux in the south. This spatial variability in particle flux to the sediment may have important consequences on benthic biota.



supplementary Figure 1 Light microscopic images of some commonly found centric and pennate diatom frustules obtained from the central Arabian Sea surface sediments. *Coscinodiscus* sp. (A-B), *Thalassiosira* sp. (C-D); *Rhizosolenia* sp. (E), *Hemidiscus* sp. (F), *Cyclotella* sp. (G), *Actinoptychus* sp. (H), *Bacillaria* sp. (I), *Fragilariopsis* sp. (J), *Fragilaria* sp.(K), *Navicula* sp (L), *Pseudo-nitzschia* sp. (M), *Nitzschia* sp. (N-O), Radiolarians (P-S) at scale bar 10 µm.